WILEY ECOLOGY

The spatial synchrony of species richness and its relationship to ecosystem stability

Journal:	*Ecology*
Manuscript ID	ECY20-1429
Wiley - Manuscript type:	Articles
Date Submitted by the Author:	08-Dec-2020
Complete List of Authors:	Walter, Jonathan; University of Virginia, Department of Environmental Sciences Shoemaker, Lauren; University of Wyoming, Botany Lany, Nina; Michigan State University, Forestry Castorani, Max; University of Virginia, Department of Environmental Sciences Fey, Samuel; Reed College, Biology Dudney, Joan; UC Berkeley, Environmental Science, Policy, and Management; University of California Davis, Department of Plant Sciences Gherardi, Laureano; Arizona State University, School of Life Sciences Portales-Reyes, Cristina; University of Minnesota, Ecology, Evolution, and Behavior Rypel, Andrew; University of California Davis, Wildlife, Fish & Conservation Biology Cottingham, Kathryn; Dartmouth College, Biological Sciences Suding, Katharine; University of Colorado, Institute of Arctic & Alpine Research; University of Colorado Boulder, Ecology and Evolutionary Biology Reuman, Daniel; University of Kansas, Ecology and Evolutionary Biology Hallett, Lauren; University of Oregon, Institute of Ecology and Evolution
Substantive Area:	Community Analysis/Structure/Stability < Community Ecology < Substantive Area, Theory < Substantive Area
Organism:	
Habitat:	
Geographic Area:	
Key words/phrases:	Spatial synchrony, biodiversity, community synchrony, ecosystem stability, dispersal, Moran effect
Abstract:	Synchrony is broadly important to population and community dynamics due to its ubiquity and implications for extinction dynamics, system stability, and species diversity. Investigations of synchrony in community ecology have tended to focus on covariance in the abundances of multiple species in a single location. Yet, the importance of regional environmental variation and spatial processes in community dynamics

	suggests that community properties, such as species richness, could fluctuate synchronously across sites in a metacommunity, in an analog of population spatial synchrony. Here, we test the prevalence of this phenomenon and the conditions under which it may occur using theoretical simulations and empirical data from 20 marine and terrestrial metacommunities. Additionally, given the importance of biodiversity for stability of ecosystem function, we posit that spatial synchrony in species richness is strongly related to stability. Our findings show that that metacommunities often exhibit spatial synchrony in species richness. We also found that richness synchrony can be driven by environmental stochasticity and dispersal, two mechanisms of population spatial synchrony. Richness synchrony also depended on community structure, including species evenness and beta diversity. Strikingly, ecosystem stability was more strongly related to richness synchrony than to species richness itself, likely because richness synchrony integrates information about community processes and environmental forcing. Our study highlights a new approach for studying spatiotemporal community dynamics and emphasize the spatial dimensions of community dynamics and stability.

The spatial synchrony of species richness and its relationship to ecosystem stability

Jonathan A. Walter[1], Lauren G. Shoemaker[2], Nina K. Lany[3], Max C. N. Castorani[1], Samuel B. Fey[4], Joan C. Dudney[5], Laureano Gherardi[6], Cristina Portales-Reyes[7], Andrew L. Rypel[8], Kathryn L. Cottingham[9], Katharine N. Suding[10], Daniel C. Reuman[11], and Lauren M. Hallett[12]

[1]Department of Environmental Sciences, University of Virginia, Charlottesville, VA
[2]Botany Department, University of Wyoming, Laramie, WY
[3]Department of Forestry, Michigan State University, East Lansing, MI
[4]Department of Biology, Reed College, Portland, OR
[5]Department of Plant Sciences, University of California-Davis, Davis, CA
[6]School of Life Sciences, Arizona State University, Tempe, AZ
[7]Department of Ecology, Evolution, and Behavior, University of Minnesota, St. Paul, MN
[8]Department of Wildlife, Fish, and Conservation Biology, University of California, Davis, CA
[9]Department of Biological Sciences, Dartmouth College, Hanover, NH
[10]Department of Ecology and Evolutionary Biology, University of Colorado, Boulder, CO
[11]Department of Ecology and Evolutionary Biology and Kansas Biological Survey, University of Kansas, Lawrence, KS
[12]Environmental Studies Program and Department of Biology, University of Oregon, Eugene, OR

Corresponding author:
Jonathan Walter
Department of Environmental Sciences
University of Virginia
291 McCormick Rd
Box 400123
Charlottesville, VA 22903, USA
jaw3es@virginia.edu
Phone:+1 434-924-3186

Data accessibility statement: This research is based on publicly available data hosted by the Environmental Data Initiative (EDI). Draft data products specific to this study are hosted at `https://portal-s.edirepository.org/nis/mapbrowse?scope=edi&identifier=436` (grasslands) and `https://portal-s.edirepository.org/nis/mapbrowse?scope=edi&identifier=437` (marine); final datasets will be permanently archived and publicly released upon manuscript acceptance. R code to reproduce this study is available during review on GitHub at `https://github.com/jonathan-walter/richness-synchrony`. Upon acceptance, the GitHub repository will be archived on Zenodo. DOIs for data and code will provided at the end of the published article.

1 Abstract

Synchrony is broadly important to population and community dynamics due to its ubiquity and implications for extinction dynamics, system stability, and species diversity. Investigations of synchrony in community ecology have tended to focus on covariance in the abundances of multiple species in a single location. Yet, the importance of regional environmental variation and spatial processes in community dynamics suggests that community properties, such as species richness, could fluctuate synchronously across sites in a metacommunity, in an analog of population spatial synchrony. Here, we test the prevalence of this phenomenon and the conditions under which it may occur using theoretical simulations and empirical data from 20 marine and terrestrial metacommunities. Additionally, given the importance of biodiversity for stability of ecosystem function, we posit that spatial synchrony in species richness is strongly related to stability. Our findings show that that metacommunities often exhibit spatial synchrony in species richness. We also found that richness synchrony can be driven by environmental stochasticity and dispersal, two mechanisms of population spatial synchrony. Richness synchrony also depended on community structure, including species evenness and beta diversity. Strikingly, ecosystem stability was more strongly related to richness synchrony than to species richness itself, likely because richness synchrony integrates information about community processes and environmental forcing. Our study highlights a new approach for studying spatiotemporal community dynamics and emphasize the spatial dimensions of community dynamics and stability.

Key words: spatial synchrony, biodiversity, community synchrony, ecosystem stability, dispersal, Moran effect

2 Introduction

Synchrony has broad importance in population and community ecology, and recent efforts that integrate perspectives from these sub-disciplines have generated new insights into spatiotemporal population and community dynamics (Wang & Loreau, 2014; Walter *et al.*, 2020; Wilcox *et al.*, 2017; Arribas *et al.*, 2019; Lee *et al.*, 2019). Population spatial synchrony, where temporal fluctuations in abundance are correlated across populations inhabiting multiple locations, is a fundamental feature of population dynamics observed across taxa and over wide-ranging spatial scales (Liebhold *et al.*, 2004; Walter *et al.*, 2017). Mechanisms underlying population spatial synchrony include dispersal, spatially correlated environmental fluctuations driving shared demographic responses (Moran effects), and interactions with a species that itself exhibits spatial synchrony (Moran, 1953; Liebhold *et al.*, 2004). Spatially synchronous populations are at greater risk of regional extirpation or extinction. This is especially true for species of conservation concern, such as stocks of exploited species (Schindler *et al.*, 2015), as simultaneous rarity reduces the population rescue effect of dispersal (Earn *et al.*, 1998; Heino, 1998).

In contrast to population spatial synchrony, community ecology tends to focus on a different kind of synchrony: correlated temporal fluctuations of multiple species' abundances in a single location. Synchrony among species in a community can alter the stability of its aggregate properties. For example, synchrony among species decreases the temporal stability of total abundance or biomass production (Micheli *et al.*, 1999; Loreau & de Mazancourt, 2008). Alternatively, stability is maintained when species fluctuate independently and especially if their fluctuations negatively covary. This negative covariance between species, commonly known as compensatory dynamics, reflects heterogeneity in species' responses to environmental drivers, possibly mediated through competitive release (Gonzalez & Loreau, 2009; Hallett *et al.*, 2017).

As exemplified via the sustained focus on metacommunity theory over the past decade (Leibold *et al.*, 2004; Leibold & Chase, 2017), there is growing recognition of the importance of spatial scaling and the interplay of local versus regional dynamics on community attributes such as biodiversity (Shoemaker & Melbourne, 2016; De Meester *et al.*, 2016) and stability (Wang & Loreau, 2014; Wang *et al.*, 2019). As many of the factors that are central to population spatial synchrony—including dispersal, temporal environmental variation, and spatial heterogeneity—have also proven important to spatiotemporal community dynamics suggests that we may, *a priori*, expect that community attributes such as biodiversity exhibit spatial synchrony, at least under some conditions. To date, however, whether community attributes commonly exhibit spatial synchrony—and if so, why—is unknown. Here, we focus on spatial synchrony in species richness and explore potential mechanisms through which richness synchrony could arise, as well as its implications.

There are several reasons to investigate synchrony in richness. Biodiversity is often associated with ecosystem function (Tilman & Downing, 1994; Schulze & Mooney, 2012; Rypel & David, 2017) and stability (Cottingham *et al.*, 2001; de Mazancourt *et al.*, 2013). Species richness is widely used to quantify biodiversity, in part because presence-absence data are more easily obtained than data on abundance, or indices thereof, needed for other measures. Furthermore, studying synchrony in numbers of species bears conceptual similarity to synchrony in numbers of individuals, as in population spatial synchrony. Finally, understanding patterns and drivers of biodiversity has importance for mitigating biodiversity loss.

Here, we consider how spatial synchrony in species richness might arise mechanistically. In a given location (e.g., a patch in a metacommunity), fluctuations in richness reflect local colonization and extinction events. Species richness could therefore exhibit spatial synchrony if colonization and extinction dynamics are themselves spatially correlated due to dispersal or underlying environmental fluctuations (Harrison & Quinn, 1989). Spatially correlated environmental fluctuations could also synchronize patch-level richness by altering available niche space (Shoemaker & Melbourne, 2016) or shifting the suite of species favored under current conditions (Pitt & Heady, 1978). We expect that Moran effects on species richness are likely given that biodiversity can fluctuate in response to climatic variation (Peco *et al.*, 1998), and that Moran effects on populations comprising the community—which are common (Liebhold *et al.*, 2004)—may manifest in community metrics.

Here, we integrate insights from a theoretical metacommunity model with a synthesis of 20 empirical metacommunities from terrestrial grassland and coastal marine biomes to examine the prevalence of spatial synchrony in species richness, the ecological factors that can promote or diminish it, and how it can provide insight into the stability of ecosystem function. Drawing on the implications of spatial synchrony for population stability, and the implications of diversity and community synchrony for ecosystem stability, we hypothesize that spatial synchrony in richness will relate strongly to ecosystem stability at the landscape scale. Specifically, we address the following research questions: 1) Do local fluctuations in species richness exhibit spatial synchrony across metacommunity patches? 2) Are the well-documented drivers of population spatial synchrony (i.e., Moran effects and dispersal) also key drivers of spatial synchrony in richness? 3) Does a community's strength of spatial synchrony of richness predict ecosystem stability and how does this compare to relationships between richness and ecosystem stability? Overall, our study demonstrates the commonness of spatial synchrony in species richness, identifies key abiotic and biotic factors that alter the degree of richness synchrony, and explores how the spatial synchrony of richness may be strongly related to the temporal stability of ecosystem properties.

3 Methods

3.1 Quantifying synchrony in community properties

Although spatial synchrony has mainly been quantified for population variables, spatial synchrony can, in principle, be quantified for any time-varying quantity with measurements taken in different places. We measured spatial synchrony of species richness as follows, and is illustrated in Supplementary Material S1. We began with data consisting of species' abundances at P locations (hereafter, plots) through time. We measured species richness of each plot at each time step to compute richness, $R_{p,t}$, where p is the plot and t is the time-step. We then linearly detrended the time series, standardized variances of each time series to one, and computed the matrix of Spearman correlations for fluctuations in richness through time between all plot pairs. Finally, the lower triangle (excluding the diagonal) of the correlation matrix was averaged to produce one representative value for each site, as commonly occurs when examining community synchrony (Hallett *et al.*, 2014; Kent *et al.*, 2007), and allows us to compare across sites.

3.2 Theoretical modelling

To examine when we expect to observe spatial synchrony of richness and what mechanisms most alter it, we applied the above workflow to simulated metacommunities. Coupling a theoretical model that incorporates known underlying mechanisms with a statistical analysis of the spatial synchrony of richness provides insight into the behavior of synchrony under different ecological mechanisms. In brief, our metacommunity model connects local patch-level dynamics to regional dynamics via global dispersal. Growth, competition, and environmental effects occur within a patch, environmental conditions of each patch vary both through space and time, and patches are connected via dispersal of individuals. Within-patch dynamics follow a multispecies, metacommunity extension of the model of Loreau and de

Mazancourt 2013, which is a discrete-time modification of classic Lotka-Volterra dynamics incorporating both demographic and environmental stochasticity (Loreau & de Mazancourt, 2008; Loreau, 2010).

First, prior to local population dynamics, global dispersal between patches occurs. Abundance after dispersal, but before population growth, is indexed as time step $t + \delta$, and is:

$$N_{s,p,t+\delta} = N_{s,p,t} - d_s N_{s,p,t} + d_s \sum_{x \neq p} \frac{N_{s,x,t}}{P-1}, \tag{1}$$

where P denotes the total number of patches in the metacommunity, and d_s is a species' stochastic dispersal rate, where the probability of a propagule successfully dispersing is binomially distributed with the probability of success equal to d_s. This approach is equivalent to modeling dispersal as a multinomial distribution with probabilities of $1-d_s$ of not dispersing and $d_s/(p-1)$ of dispersing to a patch $x = 1...P$ such that $x \neq p$ (Shoemaker & Melbourne, 2016).

Following dispersal, within a patch, p, the abundance N of each species s changes through time t according to:

$$N_{s,p,t+1} = N_{s,p,t+\delta} \exp[r_s(1 - \frac{N_{s,p,t+\delta}}{K_s} - \sum_{j \neq s} \frac{\beta_{s,j} N_{j,p,t+\delta}}{K_j}) + \sigma_{e,s}\mu_{e,p,t} + \frac{\sigma_{d,s}\mu_{d,s,p,t}}{\sqrt{N_{s,p,t+\delta}}}], \tag{2}$$

In the above equation, r is a species' intrinsic (density-independent growth rate), K is its carrying capacity in a patch, and $\beta_{s,j}$ is the competition coefficient of species j on species s. Model parameters and their values are given in Table 1.

Demographic stochasticity is incorporated as a traditional first-order normal approximation, and represents inherent variation between individuals in birth and death rates (Lande *et al.*, 2003). Here, $\sigma_{d,s}$ is the susceptibility of species s to demographic fluctuations and $\mu_{d,s,p,t}$ are independent, identically distributed normal variables with mean zero and variance one representing fluctuations through time for each species in each patch.

Environmental stochasticity is similarly incorporated through $\mu_{e,p,t}$, which represents environmental variation in each patch through time and $\sigma_{e,s}$, which quantifies the impact of environmental variation on each species s. While Loreau and de Mazancourt (2013) restricted $\mu_{e,p,t}$ to be uncorrelated, here we extend their model to allow for temporal autocorrelation in environmental conditions and variation across patches. To do so, we follow the formulation from Ripa and Lundberg (1996), where we first create a time series of regional climate conditions, c:

$$c_{t+1} = ac_t + b\phi_t. \quad (3)$$

We set the initial condition $c_0 = 0$. In eqn 3, a controls the temporal autocorrelation of the climate where $a = 0$ represents uncorrelated, white noise. When $a > 0$, successive events are more likely to be similar to other events that occur closely in time (Ripa & Lundberg, 1996). Stochastic noise $\phi_t \sim Normal(0, 1)$ is scaled by the magnitude of its effect, b. Following Ripa and Lundberg 1996, $b = (1 - a^2)^{0.5}$, which restricts $var(c)$ to be the same for all autocorrelation (a values) considered. From the time series of regional climactic conditions, we create between-patch variation that represents the degree of microhabitat variation (Ford *et al.*, 2013; Gómez-Aparicio *et al.*, 2005). To do so, $\mu_{e,p,t} \sim Normal(c_t, h)$ where h controls the variability between patches.

Using the above model, we examine the relative effects of multiple abiotic and biotic factors on the spatial synchrony of richness. We simulated metacommunities that differed in: richness of the regional species pool (S), number of patches (P), spatial heterogeneity in patch quality (h), temporal autocorrelation of the regional climate conditions (a), the effect of environmental stochasticity on species ($\sigma_{e,s}$), species' growth rates (r), species' competitive strengths ($\beta_{s,j}$), and dispersal rates (d). All variable parameters were drawn independently from the distributions in Table 1, which also includes values for non-focal parameters (e.g. $\mu_{d,s}$, K_s). We began each simulation with species' abundances set to their carrying capacities, K_s, and as the model quickly settles on its steady-state distribution, we simulated our model for 100 time steps. We used the first 50 time steps as a "burn-in" period to remove any effect of initial conditions on our analyses. The last 50 time steps were used for calculating spatial synchrony of species richness, creating time series for each simulation with length on the same order as those from our empirical analyses. We ran a total of 2500 simulations and calculated spatial synchrony in species richness and the coefficient of variation in total abundance in all simulations.

We also considered a version of the model in which population growth occurred before dispersal, but was otherwise identical.

3.3 Empirical datasets

We paired our theoretical model with a study of 20 empirical metacommunities encompassing both grassland and coastal marine habitats, primarily drawing from the United States Long Term Ecological Research Network. All datasets consisted of regularly sampled observations of species' abundance in a community for at least 6 plots and 10 years (Table 2). All datasets focused on sessile taxa in unmanipulated plots. At some sites (Konza Prairie, Jornada Experimental Range, Sevilleta, and Moorea Coral Reef), up to three distinct communities were considered separately. Communities were considered distinct on the basis of diverging habitat such as soil type or disturbance frequency, dissimilarity in species present, and the expert opinion of investigators familiar with these sites. Additional description of community dataset properties and provenance is provided in Supplementary Material S1. We included all species having non-zero abundance in at least 5% of plot-by-time combinations in order to minimize any potential bias of observational error on our results. Preliminary analyses using different thresholds from 0% (no threshold) to 10% indicated that measured spatial synchrony of richness was robust to our 5% threshold choice.

3.4 Analyses of empirical and theoretical communities

We applied parallel analyses to our model simulations and empirical data to address our research questions. We first asked whether species richness exhibits spatial synchrony (Q1). To address this question using theoretical simulations, we computed the mean richness synchrony for all 2500 simulated metacommunities and examined the distribution of theoretical richness synchrony measures. To address this question empirically, we computed the mean spatial synchrony of richness for all 20 focal metacommunity datasets and tested the statistical significance of spatial synchrony of richness for each site. Significance testing was performed by comparing empirical values to surrogate values from simulated data generated under a null hypothesis of no spatial synchrony, while preserving the temporal autocorrelation structures of the empirical data. Surrogate datasets were generated by taking the amplitude-adjusted Fourier transform (AAFT) of input species richness time series, randomizing the phases of the Fourier components so that any remaining spatial synchrony is due to chance alone, inverse transforming the data, and measuring the synchrony of the surrogates (Schreiber & Schmitz, 2000). We generated $1,000$ surrogates for each dataset, and considered richness synchrony statistically significant when the empirical value exceeded 95% of surrogates.

To determine the key drivers of spatial synchrony in richness (Q2), we used multiple linear regression to measure the combined effects of multiple predictors on the synchrony of richness. Predictors were re-scaled to have a mean of zero and standard deviation of 1 so that regression coefficients corresponded to effect sizes. In our theoretical simulations, we examined the effects of key parameters of interest that fall into three general categories: abiotic temporal factors, abiotic spatial factors, and demographic factors. Abiotic temporal factors included in our regression are the effect of temporal variation of species (env_{sd}), and temporal autocorrelation in environmental variation (a) (Table 1). Abiotic spatial factors include the total number of patches (P) and the amount of patch heterogeneity (h). Finally, we examined the effect of demographic variation, specifically in the parameters: average species' density-independent growth rates (r_{avg}), maximum competitive strength (β_{max}), and species' dispersal rates (d_s).

To answer Q2 for empirical metacommunities, we considered the following predictor variables: biome (terrestrial or marine), site extent (maximum distance between plots), species richness, evenness, beta diversity, and species turnover rate. To facilitate model-data comparisons, we also examined the effects of species richness, evenness, beta diversity, and turnover rate in simulated metacommunities. Species richness and evenness were the mean richness and evenness of individual plots, averaged across time. Spatial beta diversity was the mean Jaccard similarity (Hallett *et al.*, 2016) among plots, with the species list for each plot inclusive of all years in the time series (after removing species present in less than 5% of plot-years). Turnover rate was the average plot-level temporal turnover in species composition (Hallett *et al.*, 2016), and site extent was the maximum distance between plots, measured in kilometers, in the empirical data and the total extent of the metacommunity (i.e. number of patches) in the theory analyses.

To address whether the strength of synchrony in richness predicts ecosystem stability (Q3), we used the coefficient of variation (CV) over time of total abundance/biomass/cover as a measure of ecosystem stability. We examined how richness synchrony predicts ecosystem stability using linear regression, and compared the strength of this relationship to the relationship between ecosystem stability and: species richness, evenness, beta diversity, turnover rate, and mean population spatial synchrony averaged across all species. We focus particularly on the often-studied relationship between richness and ecosystem stability (e.g. Tilman & Downing (1994); García-Palacios *et al.* (2018)). Here, species richness is the average richness over all plots and time steps (years).

4 Results

In both our theoretical model and across 20 empirical metacommunities, spatial synchrony in species richness varied widely among communities, spanning nearly the entire plausible range of the statistic (Figure 1). The distributions of theoretical and empirical richness synchrony were qualitatively similar (Figure 1a,b). Coastal marine metacommunities tended to exhibit less richness synchrony than terrestrial grasslands, but also tended to have the larger spatial extents (Table 2). The magnitudes of spatial synchrony in richness tended to be significantly greater than surrogates representing a null hypothesis of no synchrony, suggesting that spatial synchrony of richness is a common phenomenon across ecosystems (Supplementary Material S2); in all empirical metacommunities, $p < 0.05$, with the exception of Dry Tortugas (Florida Keys) corals (DRT; $p = 0.18$) and Maui, Hawaii corals (MAU; $p = 0.052$).

When examining which parameters predominantly alter the synchrony of richness in our model, we found that temporal abiotic variation had the strongest effect, followed by demographic rates. Specifically, the effect sizes indicated that the strength of temporal environmental variation (env_{sd}) and the degree of autocorrelation in the temporal environmental fluctuations (a) had the strongest effects on richness synchrony (Fig. 2). Dispersal (d) and competitive strength (β_{max}) had smaller, but still positive effect on richness synchrony. The positive effect of dispersal was consistent with our expectations from population synchrony, where increasing dispersal increases population synchrony. Spatial heterogeneity in environmental variation exhibited a slight negative effect on richness synchrony. The direction of this effect is consistent with our expectation that Moran effects shape spatial synchrony in species richness, but its low magnitude indicates important roles for other factors. This combination of predictors explained 55% of variation in richness synchrony across 2,500 simulations.

In empirical metacommunities, biome (i.e. marine versus grassland ecosystems) was strongly related to richness synchrony, but with a large standard error (Figure 1). Because both the degree of spatial autocorrelation in environmental conditions and the rate of dispersal between plots typically decrease as the distance between plots grows, we expected that extent would have a negative effect on richness synchrony, consistent with dispersal and Moran effects acting as key drivers of richness synchrony. Consistent with our prediction, site extent was negatively related to synchrony in richness, however with a large standard error (Figure 3).

As some underlying biological and abiotic factors were impossible to measure in observational studies, we examined potential covariates of richness synchrony that can be calculated for both theoretical models and observational data, allowing us to assess model-data coherence. There was a strong positive relationship between species turnover on richness synchrony across both theoretical and empirical metacommunities (Figure 3). This is consistent with the fact that changes in species richness imply turnover, but also highlights how community structure and disturbance dynamics (Kraft *et al.*, 2011; Myers *et al.*, 2015) also likely shaped the spatial synchrony of richness. Given that some communities may be more prone to turnover than others when faced with environmental variation, communities may vary in the magnitude of spatial synchrony of richness. In empirical communities, richness synchrony was positively related to the average richness of the metacommunity, but the standard error was large; in theoretical metacommunities, the effect was small and slightly negative (Figure 3). Theoretical metacommunities exhibited a negative relationship between spatial β diversity and richness synchrony; in empirical metacommunities the parameter estimate was near zero, but with a large standard error encompassing the estimate for theoretical metacommunities. Neither model nor data show a notable effect of evenness on richness synchrony. In our simulations, these possible explanatory variables were emergent properties of underlying community assembly mechanisms, not directly controlled. This combination of predictors explained 69% of variability in richness synchrony in empirical metacommunities, and 21%

of variability in richness synchrony in simulated metacommunities.

Importantly, spatial synchrony of richness was strongly positively related to the stability of ecosystem function in both theoretical and empirical metacommunities, and exhibited a stronger relationship with the coefficient of variation (community CV) than species richness itself (Figure 4). Both theoretical and empirical relationships between the spatial synchrony of richness and community stability were strong ($R^2 = 0.48$ and $R^2 = 0.65$, respectively), especially compared to the relationship between diversity and stability ($R^2 = 0.02$ and $R^2 = 0.13$, respectively). As such, across sites and underlying mechanisms—as manipulated in our simulation modeling—the spatial synchrony of richness emerged as the stronger predictor of community stability. Additionally, the spatial synchrony of richness was generally more strongly related to stability than evenness, beta diversity, turnover rate, or mean population spatial synchrony (Supplementary Material S3). Reversing the order of dispersal and population growth in theoretical simulations yielded consistent results (Supplementary Material S4).

5 Discussion

Metacommunities often exhibit spatially synchronous fluctuations in species richness (Q1) that are driven in part by Moran effects and dispersal (Q2), two canonical drivers of population spatial synchrony (Liebhold *et al.*, 2004; Moran, 1953; Walter *et al.*, 2017). In both mathematical models and observational data spanning marine and terrestrial metacommunities, spatial synchrony of richness predicts ecosystem stability better than species richness itself (Q3), and better than a selection of other community properties with known relationships to stability. These findings integrate perspectives on spatial synchrony from population ecology with biodiversity's implications for ecosystem stability and function, and reinforce the importance of spatial dimensions of stability (Wang & Loreau, 2014; Wilcox *et al.*, 2017;

Lamy *et al.*, 2019; Gonzalez *et al.*, 2020; Wang *et al.*, 2019).

Spatial synchrony in species richness appears to be a common phenomenon. Across 20 empirical metacommunities in grassland and coastal marine habitats, spatial synchrony in richness varied substantially, but in 90% of cases, was greater than expected compared against a null hypothesis of no spatial synchrony. In addition, spatial synchrony in species richness has been documented in two other very recent studies (Barringer *et al.*, 2020; Arribas *et al.*, 2019), but these studies considered only a few empirical communities. In our study, terrestrial ecosystems tended to exhibit higher spatial synchrony in species richness, possibly due to differences across biomes in underlying community dynamics. However, marine sites also tended to have larger spatial extents (Table 2), which may partially explain this pattern due to the potential for decreased dispersal and environmental spatial correlation with increasing spatial extent. The biomes also tended to differ in the typical lifespans of individuals in the community (e.g. long-lived corals vs. a mix of annual and perennial plants), possibly affecting the sensitivity of the community to interannual environmental variability.

The variability in the degree of spatial synchrony of richness exhibited by a metacommunity was influenced by attributes of the environment, especially the degree of temporal variability in environmental conditions, and by the structure of the community. Fluctuations in species richness imply year-to-year species turnover, and some communities will be more prone to turnover than others due to underlying environmental conditions, disturbance events (Worm & Duffy, 2003; Myers *et al.*, 2015), and the demography of constituent species (Ripa & Lundberg, 1996; Adler & Drake, 2008). How demography alters richness synchrony likely interacts with the nature of environmental fluctuations. Some communities with many rare, extinction-prone species could actually exhibit little richness synchrony if extinctions are spatiotemporally random, e.g. if they arise more so from demographic stochasticity than environmental forcing. By contrast, a community with lower turnover might exhibit greater synchrony in richness if species turnover is closely tied to large, spatially synchronous environmental perturbations that locally extirpate, or facilitate the emergence of, multiple species simultaneously.

In fact, the dependence of richness synchrony on both environmental variation and community structure seems to explain small discrepancies between our theoretical and empirical results. In contrast to our empirical metacommunities, which showed a strong negative relationship between site extent on richness synchrony, the effects of dispersal and in particular Moran effects (patch heterogeneity) in simulated metacommunities were relatively weak (Figures 2, 3). Additionally, species richness had opposing relationships with richness synchrony in empirical versus theoretical cases. In empirical metacommunities, turnover was higher than simulated communities, and richness and evenness were positively correlated, suggesting that as we added more species the aggregated community-level carrying capacity was partitioned among more species; this lowered abundances on average, making more species susceptible to environmental perturbation and leading to synchronous fluctuations in richness. Meanwhile, in our simulated metacommunities, turnover rates were low and evenness was high but negatively correlated with richness. In this case, higher richness yielded more rare species that tended to stochastically and asynchronously become locally extinct and/or colonize new patches.

The relationship between biodiversity and stability of ecosystem function has generated a great deal of interest in ecology over multiple decades of research (Tilman & Downing, 1994; Schulze & Mooney, 2012; Cottingham *et al.*, 2001; de Mazancourt *et al.*, 2013). We found that spatial synchrony in richness was more strongly related to stability of total biomass production than was species richness itself (Figure 4). The relative success of the spatial synchrony of richness in predicting ecosystem stability seems to arise primarily because it is a metric that simultaneously reflects information both about community structure and environmental variability. Our study suggests that richness synchrony may generally be closely related to ecosystem stability and function, providing additional insight into the relationship between biodiversity, synchrony, and stability.

Studying the spatial synchrony of species richness represents a promising approach for investigating drivers of community variability and their consequences for stability of ecosystem function. We note that our approach could also be used to investigate spatial synchrony in other community metrics, such as the turnover rate or Shannon's diversity index. Although the causes of spatial synchrony in species richness appear complex and remain only partly understood, richness synchrony appears to be an effective integrator of several processes linking biodiversity and system stability. While investigations of the spatial synchrony of community variables are uncommon now, the growing availability of long-term, spatially replicated community datasets enables broader application of this approach. Species richness may be particularly amenable in this regard since presence-absence data may be obtained more easily than the abundances of a full species assemblage. Additionally, geographic and timescale-specific approaches that have produced gains in understanding of population spatial synchrony (Walter *et al.*, 2017; Sheppard *et al.*, 2016) likely have similar potential for understanding patterns and drivers of variability in communities, their ability in inferring underlying community assembly and coexistence dynamics, and importance for ecosystem stability. These same approaches may prove invaluable in understanding the scale-dependence of ecological stability (Chase & Ryberg, 2004; Wang & Loreau, 2014; Gonzalez *et al.*, 2020; Downing *et al.*, 2008).

6 Acknowledgements

This work is a product of the LTER Synchrony Synthesis working group hosted at National Center for Ecological Analysis and Synthesis (NCEAS) and funded by the National Science Foundation under grant DEB-1545288 through the LTER Network Communications Office.

The authors acknowledge the Minnesota Supercomputing Institute (MSI) at the University of Minnesota for providing resources that contributed to the research results reported within this paper. JAW was supported by USDA-NIFA 2016-67012-24694, The Nature Conservancy, and the University of Virginia. LGS was supported by the James S. McDonnell Foundation grant 220020513. Significant funding for data collection was provided by the National Science Foundation (NSF) through the LTER network grant numbers: DEB-9411971, DEB 0080412, DEB-0917668, DEB-1235828 & DEB-1242747 (JRN); DEB-0620482 (SEV); DEB-1440484 (KNZ); OCE-9982105, OCE-0620276, OCE-1232779, & OCE-1831937 (SBC); OCE-0417412, OCE-1026851, OCE-1236905 (MCR); DEB-0343570, DEB-0841441, & DEB-1350146 (USVI). Additional funding for data collection was provided by the United States Geologic Survey, the University of Puerto Rico Sea Grant, and the Office of Naval Research. E. Defriez, L. Sheppard, S. Wang and L. Zhao contributed to discussions of this work.

References

Adler, P. B. & Drake, J. M. (2008). Environmental variation, stochastic extinction, and competitive coexistence. *The American Naturalist*, 172, E186–E195.

Arribas, L. P., Gutierrez, J. L., Bagur, M., Soria, S. A. & Penchaszadeh, P. E. (2019). Variation in aggregate descriptors of rocky shore communities: a test of synchrony across spatial scales. *Marine Biology*, 166, 44.

Barringer, B. C., Koenig, W. D., Pearse, I. S. & Knops, J. M. H. (2020). Population ecology and spatial synchrony in the abundance of leaf gall wasps within and among populations of valley oak (quercus lobata). *Population Ecology*.

Chase, J. M. & Ryberg, W. A. (2004). Connectivity, scale-dependence, and the productivity-diversity relationship. *Ecology Letters*, 7, 676–683.

Cottingham, K. L., Brown, B. L. & Lennon, J. T. (2001). Biodiversity may regulate the temporal variability of ecological systems. *Ecology Letters*, 4, 72–85.

de Mazancourt, C., Isbell, F., Larocque, A., Berendse, F., De Luca, E., Grace, J. B., Haegeman, B., Polley, W., Roscher, C., Schmid, B., Tilman, D., van Ruijven, J., Weigelt, A., Wilsey, B. J. & Loreau, M. (2013). Predicting ecosystem stability from community composition and biodiversity. *Ecology Letters*, 16, 617–625.

De Meester, L., Vanoverbeke, J., Kilsdonk, L. J. & Urban, M. C. (2016). Evolving perspectives on monopolization and priority effects. *Trends in Ecology & Evolution*, 31, 136–146.

Downing, A. L., Brown, B. L., Perrin, E. M., Keitt, T. H. & Leibold, M. A. (2008). Environmental fluctuations indice scale-dependent compensation and increase stability in plankton ecosystems. *Ecology*, 89, 3204–3214.

Earn, D. J. D., Rohani, P. & Grenfell, B. T. (1998). Persistence, chaos and synchrony in ecology and epidemiology. *Proc. R. Soc. Lond. B*, 265, 7–10.

Ford, K. R., Ettinger, A. K., Lundquist, J. D., Raleigh, M. S. & Lambers, J. H. R. (2013). Spatial heterogeneity in ecologically important climate variables at coarse and fine scales in a high-snow mountain landscape. *PloS One*, 8, e65008.

García-Palacios, P., Gross, N., Gaitán, J. & Maestre, F. T. (2018). Climate mediates the biodiversity–ecosystem stability relationship globally. *Proceedings of the National Academy of Sciences*, 115, 8400–8405.

Gómez-Aparicio, L., Gómez, J. M. & Zamora, R. (2005). Microhabitats shift rank in suitability for seedling establishment depending on habitat type and climate. *Journal of Ecology*, 93, 1194–1202.

Gonzalez, A., Germain, R. M., Srivastava, D. S., Filotas, E., Dee, L. E., Gravel, D., Thompson, P. L., Isbell, F., Wang, S., Kefi, S., Montoya, J., Zelnik, Y. R. & Loreau, M. (2020). Scaling-up biodiversity-ecosystem functioning research. *Ecology Letters*.

Gonzalez, A. & Loreau, M. (2009). The causes and consequences of compensatory dynamics in ecological communities. *Annu. Rev. Ecol. Evol. Syst.*, 40, 393–414.

Hallett, L. M., Hsu, J. S., Cleland, E., Collins, S. L., Dickson, T. L., Farrer, E. C., Gherardi, L. A., Gross, K. L., Hobbs, R. J., Turnbull, L. & Suding, K. N. (2014). Biotic mechanisms of community stability shift along a precipitation gradient. *Ecology*, 95, 1693–1700.

Hallett, L. M., Jones, S. K., MacDonald, A. A. M., Jones, M. B., Flynn, D. F. B., Ripplinger, J., Slaughter, P., Gries, C. & Collins, S. L. (2016). Codyn: an r package of community dynamics metrics. *Methods in Ecology and Evolution*, 7, 1146–1151.

Hallett, L. M., Stein, C. & Suding, K. N. (2017). Functional diversity increases ecological stability in a grazed grassland. *Oecologia*, 183, 831–840.

Harrison, S. & Quinn, J. F. (1989). Correlated environments and the persistence of metapopulations. *Oikos*, XX, 293–298.

Heino, M. (1998). Noise colour, synchrony and extinctions in spatially structured populations. *Oikos*, 83, 368–375.

Kent, A. D., Yannarell, A. C., Rusak, J. A., Triplett, E. W. & McMahon, K. D. (2007). Synchrony in aquatic microbial community dynamics. *The ISME journal*, 1, 38.

Kraft, N. J., Comita, L. S., Chase, J. M., Sanders, N. J., Swenson, N. G., Crist, T. O., Stegen, J. C., Vellend, M., Boyle, B., Anderson, M. J. *et al.* (2011). Disentangling the drivers of β diversity along latitudinal and elevational gradients. *Science*, 333, 1755–1758.

Lamy, T., Wang, S., Renard, D., Lafferty, K. D., Reed, D. C. & Miller, R. J. (2019). Species insurance trumps spatial insurance in stabilizing biomass of a marine macroalgal metacommunity. *Ecology*, e02719.

Lande, R., Engen, S. & Saether, B.-E. (2003). *Stochastic population dynamics in ecology and conservation*. Oxford University Press on Demand.

Lee, A. M., Saether, B.-E. & Engen, S. (2019). Spatial covariation of competing species in a fluctuating environment. *Ecology*.

Leibold, M. A. & Chase, J. M. (2017). *Metacommunity ecology*, vol. 59. Princeton University Press.

Leibold, M. A., Holyoak, M., Mouquet, N., Amarasekare, P., Chase, J. M., Hoopes, M. F., Holt, R. D., Shurin, J. B., Law, R., Tilman, D. *et al.* (2004). The metacommunity concept: a framework for multi-scale community ecology. *Ecology letters*, 7, 601–613.

Liebhold, A., Koenig, W. D. & Bjørnstad, O. N. (2004). Spatial synchrony in population dynamics. *Annu. Rev. Ecol. Evol. Syst.*, 35, 467–490.

Loreau, M. (2010). *From populations to ecosystems: Theoretical foundations for a new ecological synthesis (MPB-46)*, vol. 50. Princeton University Press.

Loreau, M. & de Mazancourt, C. (2008). Species synchrony and its drivers: neutral and nonneutral community dynamics in fluctuating environments. *The American Naturalist*, 172, E48–E66.

Loreau, M. & de Mazancourt, C. (2013). Biodiversity and ecosystem stability: a synthesis of underlying mechanisms. *Ecology letters*, 16, 106–115.

Micheli, F., Cottingham, K. L., Bascompte, J., Eckert, G. L., Fischer, J. M., Keitt, T. H., Kendall, B. E., Klug, J. L. & Rusak, J. A. (1999). The dual nature of community variability. *Oikos*, 85, 161–169.

Moran, P. A. P. (1953). The statistical analysis of the canadian lynx cycle ii. synchronization and meteorology. *Australian Journal of Ecology*, 1, 291–298.

Myers, J. A., Chase, J. M., Crandall, R. M. & Jiménez, I. (2015). Disturbance alters beta-diversity but not the relative importance of community assembly mechanisms. *Journal of Ecology*, 103, 1291–1299.

Peco, B., Espigares, T. & Levassor, C. (1998). Trends and fluctuations in species abundance and richness in mediterranean annual pastures. *Applied Vegetation Science*, 1, 21–28.

Pitt, M. & Heady, H. (1978). Responses of annual vegetation to temperature and rainfall patterns in northern california. *Ecology*, 59, 336–350.

Ripa, J. & Lundberg, P. (1996). Noise colour and the risk of population extinctions. *Proc. R. Soc. Lond. B*, 263, 1751–1753.

Rypel, A. L. & David, S. R. (2017). Pattern and scale in latidude-production relationships for freshwater fishes. *Ecosphere*, 8, e01660.

Schindler, D. E., Armstrong, J. B. & Reed, T. E. (2015). The portfolio concept in ecology and evolution. *Frontiers in Ecology and the Environment*, 13, 257–263.

Schreiber, T. & Schmitz, A. (2000). Surrogate time series. *Physica D*, 142, 346–382.

Schulze, E.-D. & Mooney, H. A. (2012). *Biodiversity and ecosystem function.* Springer Science and Business Media.

Sheppard, L. W., Bell, J. R., Harrington, R. & Reuman, D. C. (2016). Changes in large-scale climate alter spatial synchrony of aphid pests. *Nature Climate Change*, 6, 610–613.

Shoemaker, L. G. & Melbourne, B. A. (2016). Linking metacommunity paradigms to spatial coexistence mechanisms. *Ecology*, 97, 2436–2446.

Tilman, D. & Downing, J. A. (1994). Biodiversity and stability in grasslands. *Nature*, 367, 363–365.

Walter, J. A., Hallett, L. M., Sheppard, L. W., Anderson, T. L., Zhao, L., Hobbs, R. J., Suding, K. N. & Reuman, D. C. (2020). Micro-scale geography of synchrony in a serpentine plant community. *Journal of Ecology*.

Walter, J. A., Sheppard, L. W., Anderson, T. L., Kastens, J. H., Bjørnstad, O. N., Liebhold, A. M. & Reuman, D. C. (2017). The geography of spatial synchrony. *Ecology Letters*, 20, 801–814.

Wang, S., Lamy, T., Hallett, L. M. & Loreau, M. (2019). Stability and synchrony across ecological hierarchies in heterogeneous metacommunities: linking theory to data. *Ecography*, 42, 1200–1211.

Wang, S. & Loreau, M. (2014). Ecosystem stability in space: alpha, beta, and gamma variability. *Ecology Letters*, 17, 891–901.

Wilcox, K. R., Tredennick, A. T., Koerner, S. E., Grman, E., Hallett, L. M., Avolio, M. L., La Pierre, K. J. & et. al. (2017). Asynchrony among local communities stabilizes ecosystem function of metacommunities. *Ecology Letters*, 20, 1534–1545.

Worm, B. & Duffy, J. E. (2003). Biodiversity, productivity and stability in real food webs. *Trends in Ecology & Evolution*, 18, 628–632.

Table 1: Model parameters, description, and ranges used in generating simulations.

Parameter	Description	Value/Range
S	number of species in the regional species pool	Sample(min= 30, max= 130)
P	number of patches in the metacommunity	Sample(min= 10, max= 90)
h	spatial heterogeneity between patches	Uniform(min= 0, max= 0.5)
a	temporal autocorrelation in climate	Uniform(min= 0, max= 0.75)
b	magnitude of the effect of climate	$(1 - a^2)^{0.5}$
$\mu_{e,p,t}$	environmental fluctuations in each patch	Normal(mean= c_t, sd= h)
env_{sd}	standard deviation of effect of env. variation	Uniform(min= 0.05, max= 0.5)
$\sigma_{e,s}$	response of each species to env. variation	Normal(mean= 0, sd=env_{sd})
$\mu_{d,s,p,t}$	demographic fluctuations	Normal(mean= 0, sd= 1)
$\sigma_{d,s}$	effect of demographic fluctuations	Uniform(min= 0, max= 0.75)
r_{avg}	scaled average growth rate	Uniform(min= 0, max= 0.25)
r_i	species-specific growth rate	Uniform(min= $0.5 - r_{avg}$, max= $0.5 + r_{avg}$)
β_{max}	maximum competition coefficient	Uniform(min= 0, max= 0.05)
$\beta_{s,j}$	competition coefficient of species j on species s	Uniform(min= 0, max= β_{max})
d	dispersal rate	Uniform(min= 0, max= 0.5)
K_s	carrying capacity	Lognormal(logmean= 3, Logsd= 1)

Table 2: Empirical datasets. Dataset codes correspond to, respectively: DRT, Dry Tortugas, FL; HAY, Hayes, KS; JRG, Jasper Ridge, CA; JRN_BASN, Jornada LTER Basin plots; JRN_IBPE Jornada LTER International Biological Program exclosure plots; JRN_SUMM Jornada LTER Mount Summerford plots; KNZ_UP, Konza Prairie upland plots; KNZ_LOW, Konza Prairie lowland plots; LOK, Lower Florida Keys; MAU, Maui, HI; MCR_BACK, Moorea Coral Reef LTER Backreef plots; MCR_FRNG, Moorea Coral Reef LTER fringing reef plots; MCR_OUT, Moorea Coral Reef outer reef plots; MDK, Middle Florida Keys; SBC, Santa Barbrara Coastal LTER; SEV_B, Sevilleta LTER blue gramma plots; SEV_C, Sevilleta LTER creosotebush plots; SEV_G, Sevilleta LTER black gramma plots; UPK, Upper Florida Keys; USVI, US Virgin Islands LTER. *Year* corresponds to the initial year of the time series. *Extent* gives the maximum inter-plot distance, in km. N_{taxa} gives the total number of taxa (i.e., γ-diversity) of the site.

Dataset	Year	Length	N_{plots}	Extent	Biome	N_{taxa}	Variable	Plot size
DRT	2005	11	6	16.5	marine	25	% cover	$0.25m^2$
HAY	1943	30	13	0.05	grassland	16	% cover	$1m^2$
JRG	1983	34	12	0.03	grassland	25	% cover	$1m^2$
JRN_BASN	1989	24	49	0.09	grassland	44	biomass	$1m^2$
JRN_IBPE	1989	24	49	0.08	grassland	51	biomass	$1m^2$
JRN_SUMM	1989	24	49	0.09	grassland	53	biomass	$1m^2$
KNZ_UP	1983	33	20	0.17	grassland	47	% cover	$10m^2$
KNZ_LOW	1983	33	20	0.23	grassland	44	% cover	$10m^2$
LOK	1996	20	14	49.0	marine	28	% cover	$0.25m^2$
MAU	2001	16	9	50.4	marine	21	% cover	$0.25m^2$
MCR_BACK	2006	10	30	16.65	marine	15	% cover	$0.25m^2$
MCR_FRNG	2006	10	30	15.67	marine	28	% cover	$0.25m^2$
MCR_OUT	2006	10	30	17.29	marine	25	% cover	$0.25m^2$
MDK	1996	20	8	55.4	marine	24	% cover	$0.25m^2$
SBC	2001	18	34	73.38	marine	30	biomass	$80m^2$
SEV_B	2002	13	30	0.70	grassland	42	biomass	$1m^2$
SEV_C	1999	16	30	1.33	grassland	29	biomass	$1m^2$
SEV_G	1999	16	22	0.81	grassland	27	biomass	$1m^2$
UPK	1996	20	10	44.7	marine	23	% cover	$0.25m^2$
USVI	1992	26	6	1.38	marine	17	% cover	$0.25m^2$

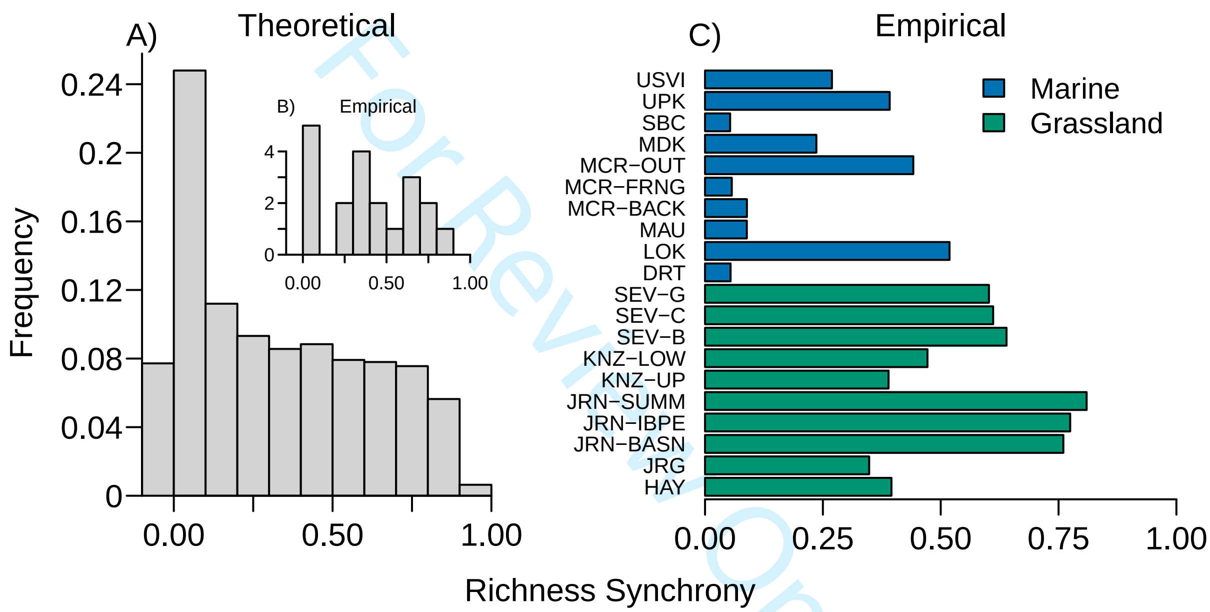

Figure 1: Spatial synchrony in species richness in (A) 2500 simulated and (B, C) 20 empirical metacommunities.

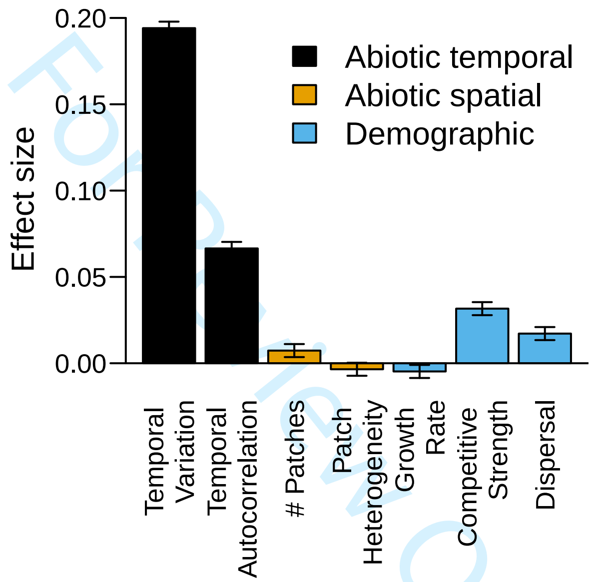

Figure 2: Effect sizes of variation in model parameters on the degree of spatial synchrony of richness in simulated metacommunities. Effect sizes are linear regression coefficients on standardized predictors. Error bars indicate 1 standard error.

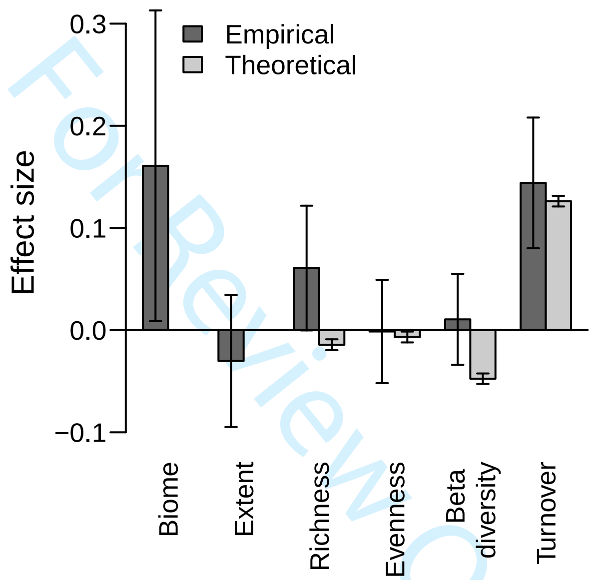

Figure 3: Effect sizes of variation in attributes of empirical and theoretical metacommunities on spatial synchrony of richness. Effect sizes are linear regression coefficients on standardized predictors. There is no direct analog of biome or extent in our theoretical simulations, so no bar is drawn. Error bars indicate 1 standard error.

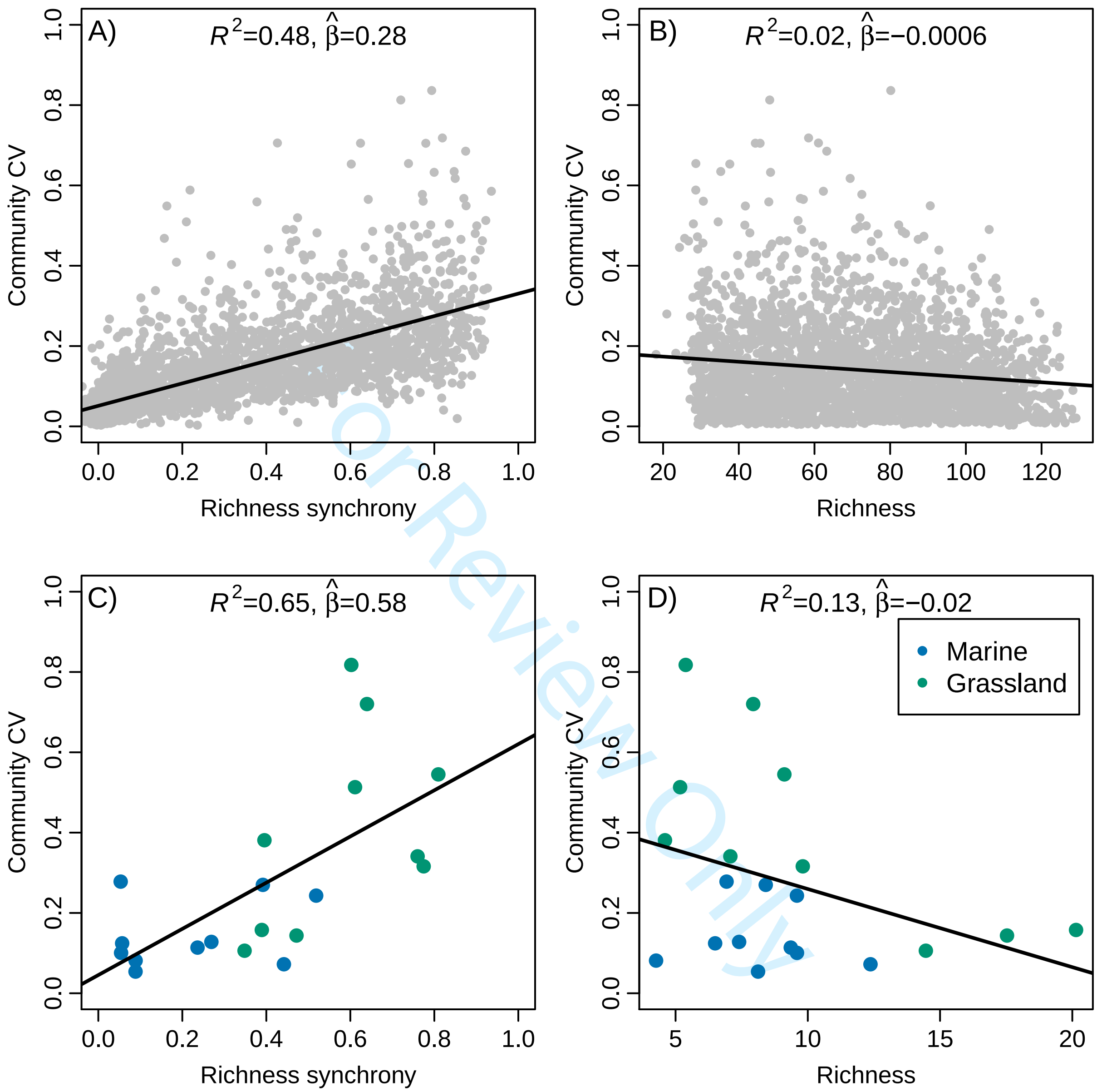

Figure 4: Richness synchrony is related to (in)stability of ecosystem function in theoretical (A) and empirical (C) metacommunities, and more strongly so than species richness itself in both theoretical (B) and empirical (D) metacommunities. The community CV is measured, for simulations, as the cv of total abundance, and for empirical datasets as the coefficient of variation of total biomass or total cover, depending on units of the underlying data (Table 2).

Supplementary materials to: The spatial synchrony of species richness and its relationship to ecosystem stability

Jonathan A. Walter, Lauren G. Shoemaker, Nina K. Lany, Max C. N. Castorani, Samuel B. Fey, Joan C. Dudney, Cristina Portales-Reyes, Andrew L. Rypel, Kathryn L. Cottingham, Katharine N. Suding, Daniel C. Reuman, Lauren M. Hallett

Correspondence: Jonathan Walter, jaw3es@virginia.edu

S1 Dataset descriptions

Data comprise the abundance (measured as percent cover or biomass) of sessile taxa measured on fixed area, permanent quadrats. Each dataset was prepared by retaining only plots that were sampled in all years and were not part of an experimental treatment, removing entries for unknown taxa, and separating into separate datasets for different communities if applicable. In cases where quadrats were not permanently marked, but rather were laid out randomly each sampling interval, abundances within each quadrat were aggregated to level of the unit of observation over time (typically the transect level). Taxa were identified to the genus or species level. We removed very rare taxa that did not occur in at least 5% of all plot-year combinations. We visually evaluated temporal changes in richness as well as species accumulation curves in both time and space.

S1.1 Florida Keys (DRT, LOK, MDK, UPK)

Data on the percent cover of corals in in Florida (Dry Tortugas National Park [DRT], Lower Florida Keys [LOK], Middle Florida Keys [MDK], and Upper Florida Keys [UPK]) were downloaded from the U.S. Geological Survey (Guest et al., 2018). At each of 40 sites, coral cover was estimated annually (1996-2015) within 2-4 permanent transects per site (40 cm wide by 22 m long), with each transect separated by 1 m. Each site represented one of three possible habitats (deep forereef,

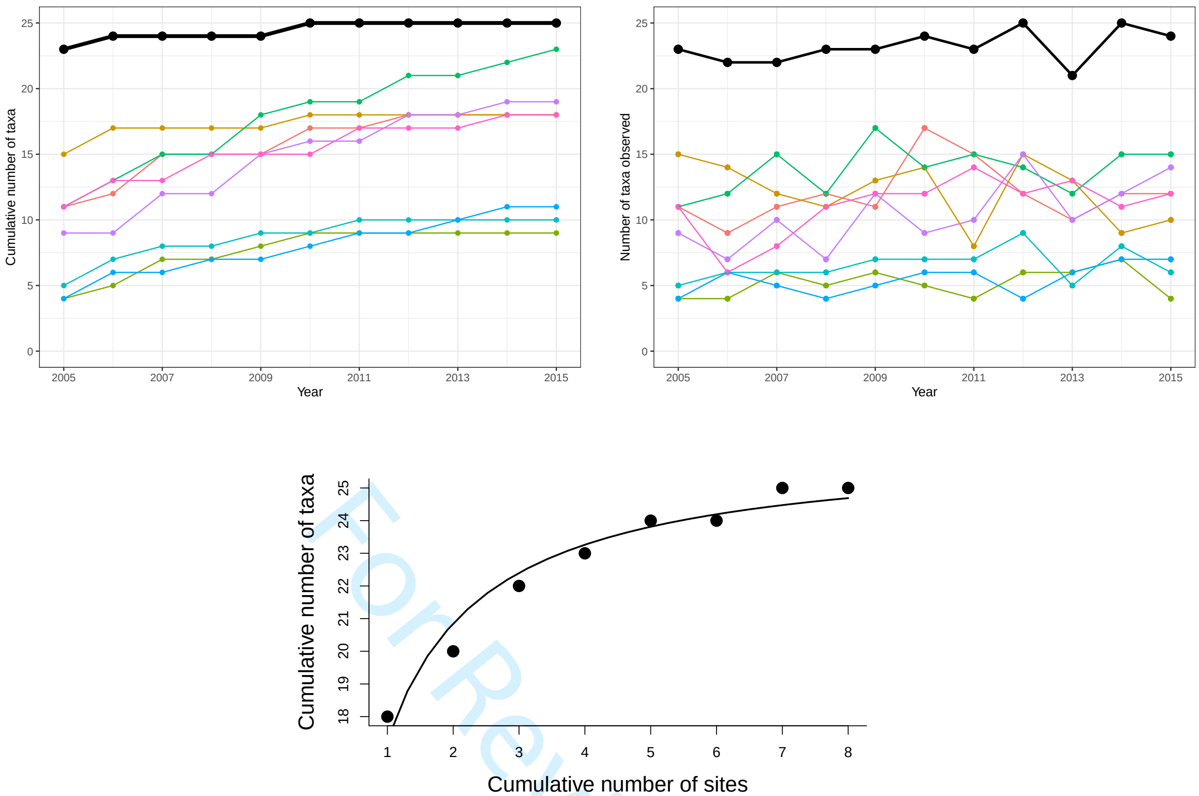

Figure S1: Temporal species accumulation curves (upper left), annual richness (upper right), and spatial species accumulation curve (lower) for 6 Dry Tortugas, Florida Keys corals plots (2005-2015). The black lines represent total site-level values across all plots.

shallow forereef, and patch reef). Cover was aggregated to the site scale. Data are shown in Figures S1-S4.

S1.2 Hayes, Kansas (HAY)

Data on plant percent cover were obtained for 13 $1m^2$ quadrats in mixed grass prairie habitat at Hay, Kansas over the period 1943-1972 (Adler et al., 2007). Taxa were identified to the species level. Data are shown in Figure S5.

S1.3 Jasper Ridge (JRG)

Jasper Ridge Biological Preserve is a serpentine grassland. Data consist of percent cover for 25 grasses and forbs identified to the species level from a long-term experiment begun in 1983 (Hobbs

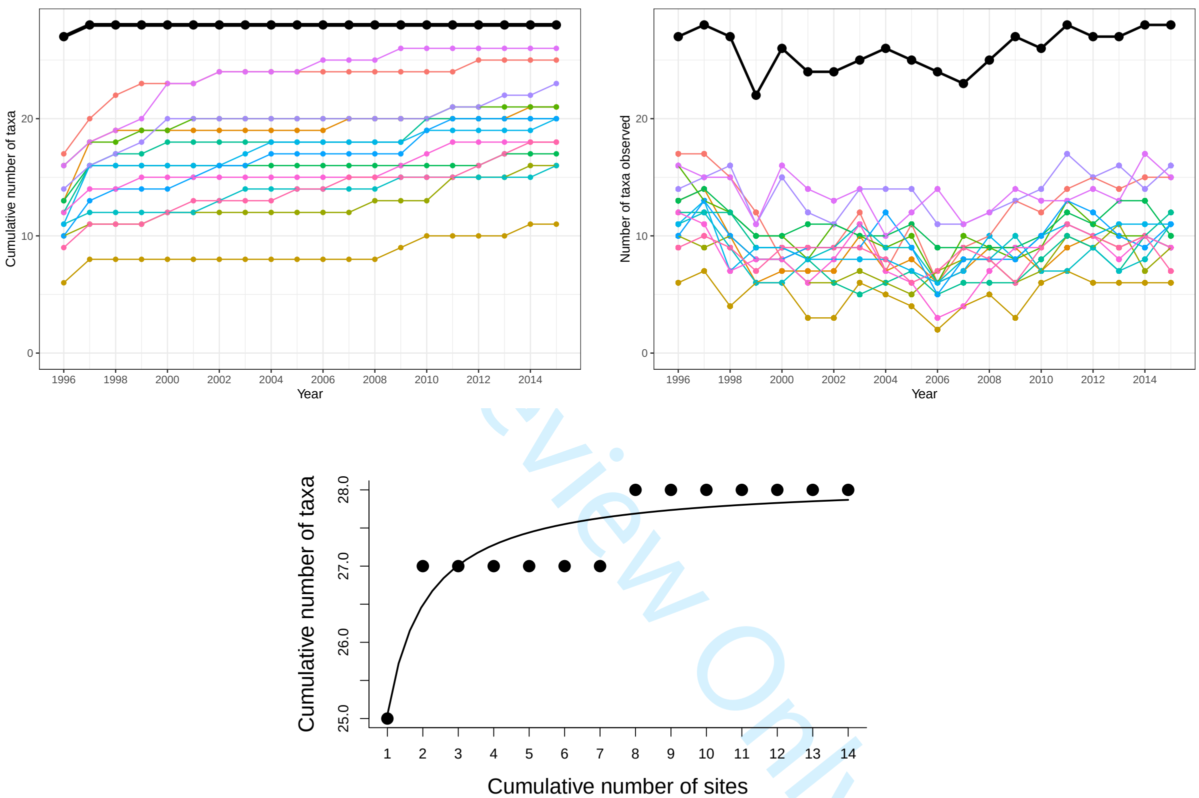

Figure S2: Temporal species accumulation curves (upper left), annual richness (upper right), and spatial species accumulation curve (lower) for 14 Lower Florida Keys corals plots (1996-2015). The black lines represent total site-level values across all plots.

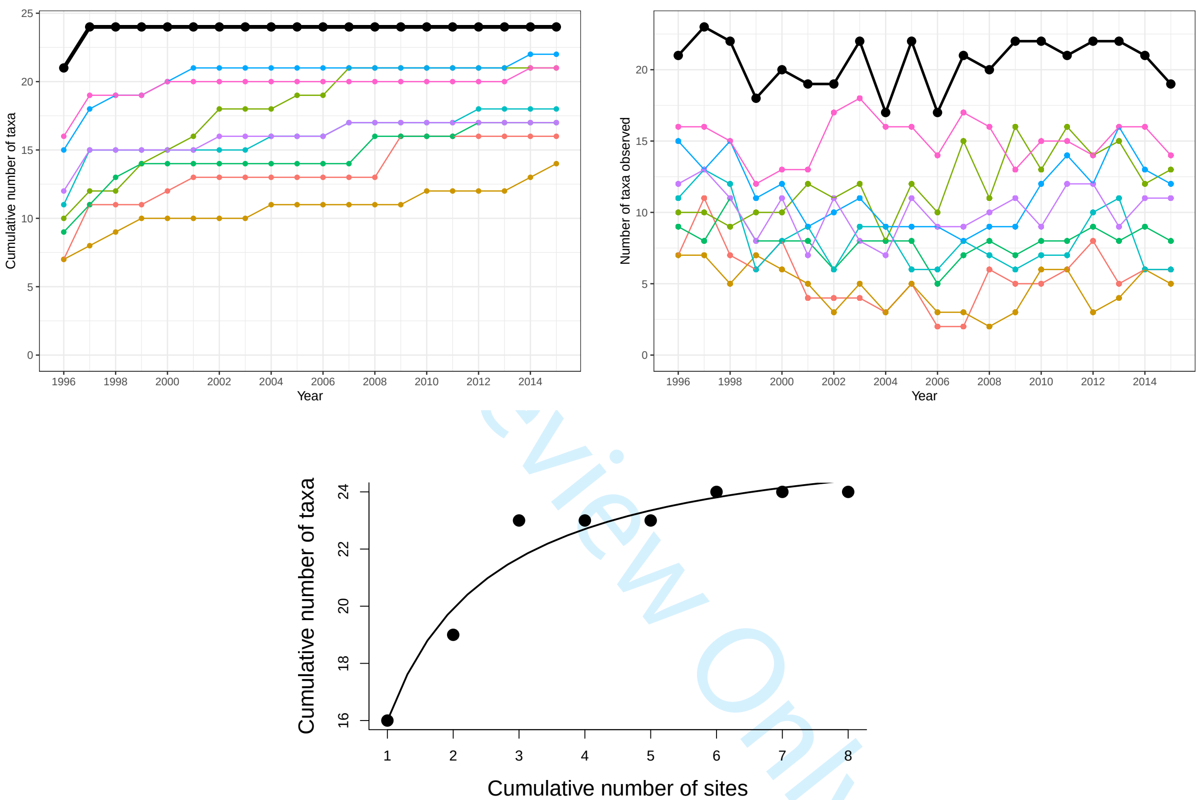

Figure S3: Temporal species accumulation curves (upper left), annual richness (upper right), and spatial species accumulation curve (lower) for 8 Middle Florida Keys corals plots (1996-2015). The black lines represent total site-level values across all plots.

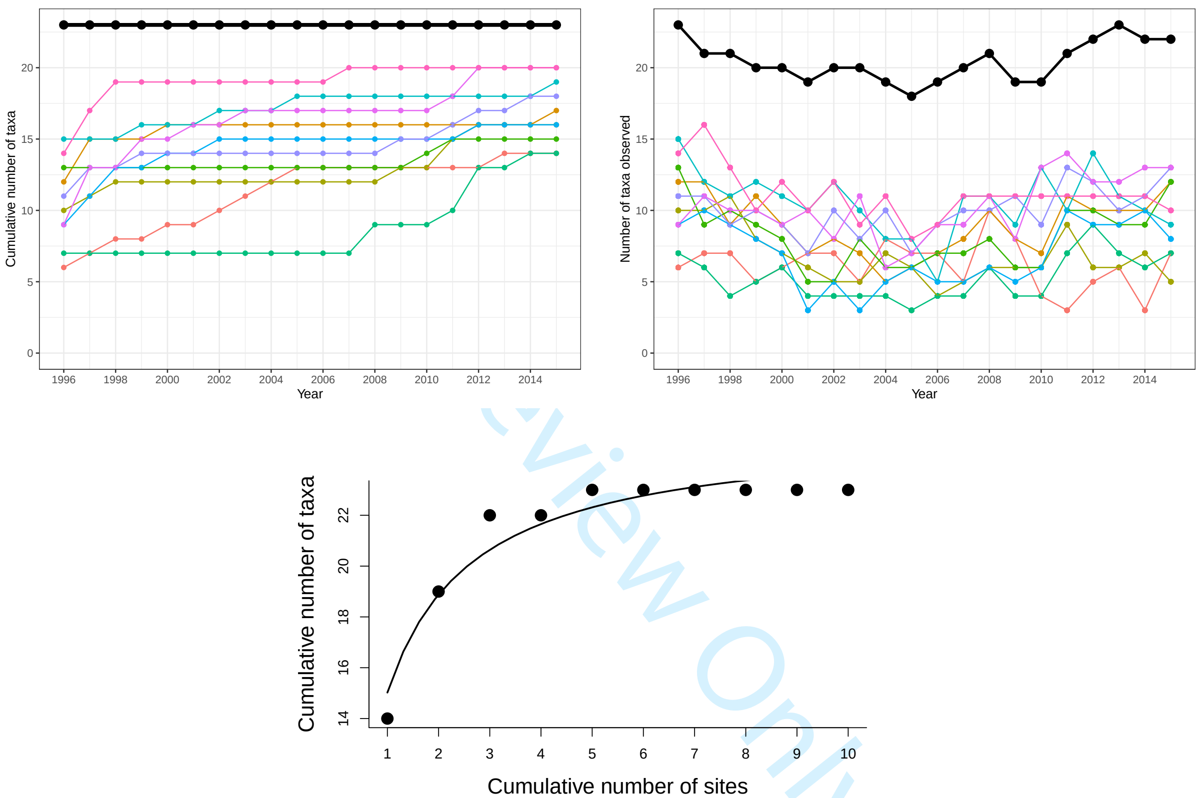

Figure S4: Temporal species accumulation curves (upper left), annual richness (upper right), and spatial species accumulation curve (lower) for 10 Upper Florida Keys corals plots (1996-2015). The black lines represent total site-level values across all plots.

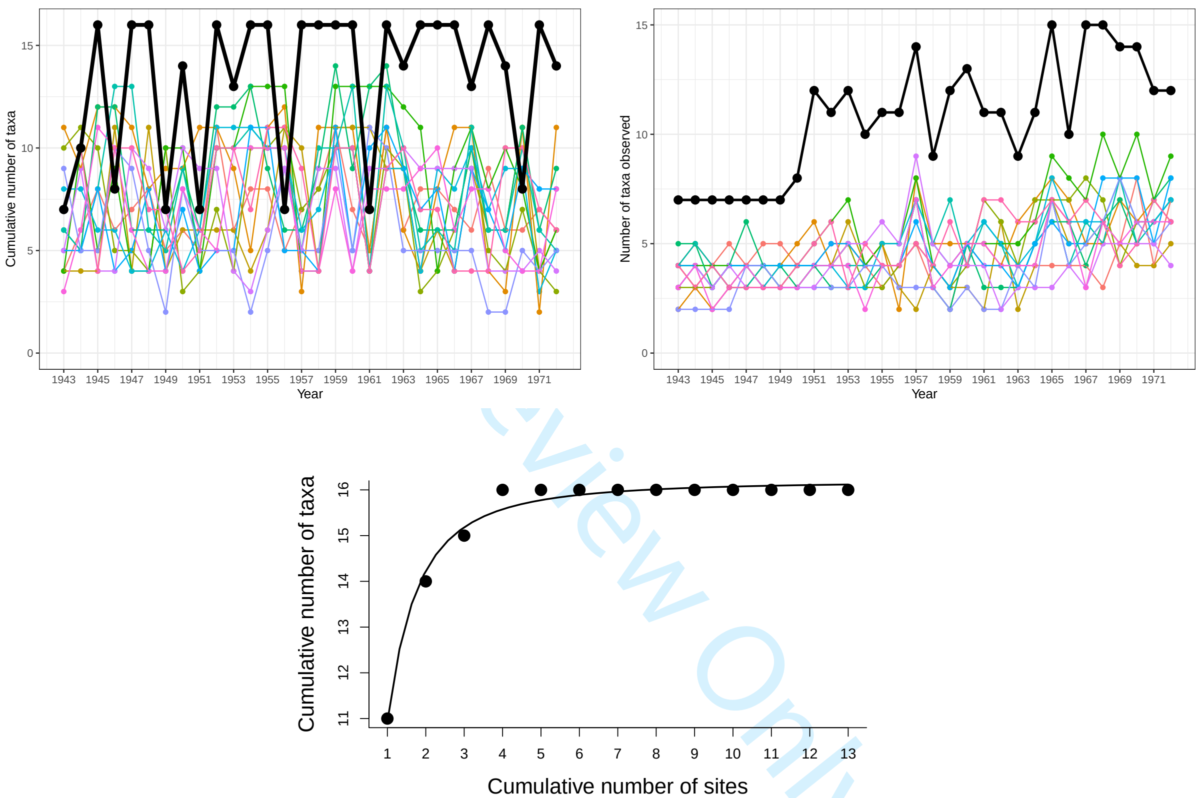

Figure S5: Temporal species accumulation curves (upper left), annual richness (upper right), and spatial species accumulation curve (lower) for 13 plots at Hay, Kansas (1943-1972). The black lines represent total site-level values across all plots.

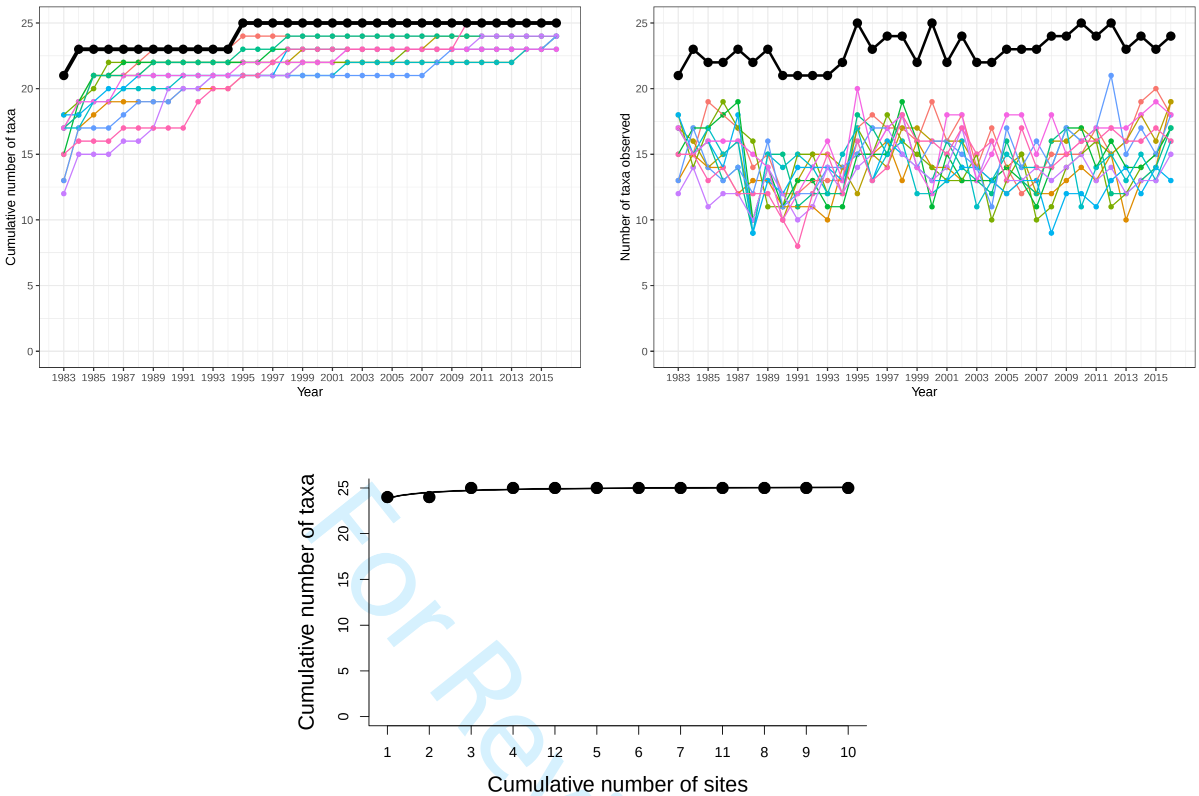

Figure S6: Temporal species accumulation curves (left), annual richness (right), and spatial species accumulation curve (lower) for 12 plots at Jasper Ridge, CA (1983-2016). The black lines represent total site-level values across all plots.

and Mooney, 1985) and sampled continuously on an annual time interval. The experiment consists of control, gopher exclosure, and rabbit exclosure plots in a nested block design: there are three replicates of each treatment and four $1m^2$ plots within each replicate. Data were obtained from Lauren Hallett on May 11, 2017. We analyzed plots in the control treatment only and considered the $1m^2$ plots the spatial unit of interest, for a total of 12 plots from 1983 to 2016 (Figure S6).

S1.4 Jornada (JRN)

Data on the biomass of plant species at the Jornada LTER through 2014 were obtained from Peters and Huenneke (2015). The grassland habitat was chosen at Jornada to be consistent across LTER site comparisons and exclude primarily shrub-dominated ecosystems. Within the grassland, 3 projects were included: BASN, IBPE, and SUMM, which are denoted as three distinct communities

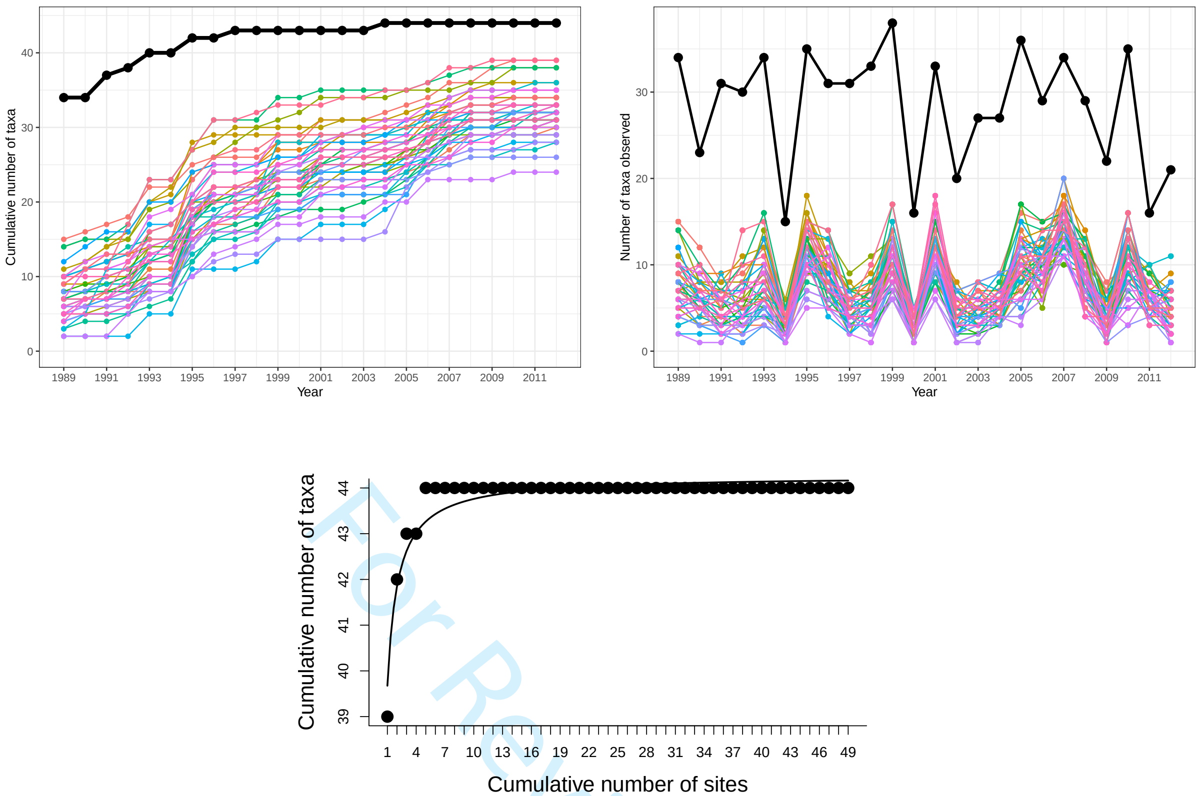

Figure S7: Temporal species accumulation curves (left), annual richness (right), and spatial species accumulation curve (lower) for 49 plots comprising the Basin (BASN) grassland community at Jornada LTER (1989-2012). The black lines represent total site-level values across all plots.

and analyzed separately. All 49 plots within each habitat type were included in our analyses and all sampling intervals between 1989 and 2012 (Figures S7, S8, and S9).

S1.5 Konza (KNZ)

Data on percent canopy cover were recorded in two different soil types in in watershed 001d (Hartnett and Collins, 2016) We analyzed the data from the the fertile, nonrocky tully (lowland) and shallow, rocky florence (upland) soil types separately. The spatial and temporal species accumulation curves level off, indicating that the community is well sampled and new species are not immigrating into the community (Figures S10 and S11).

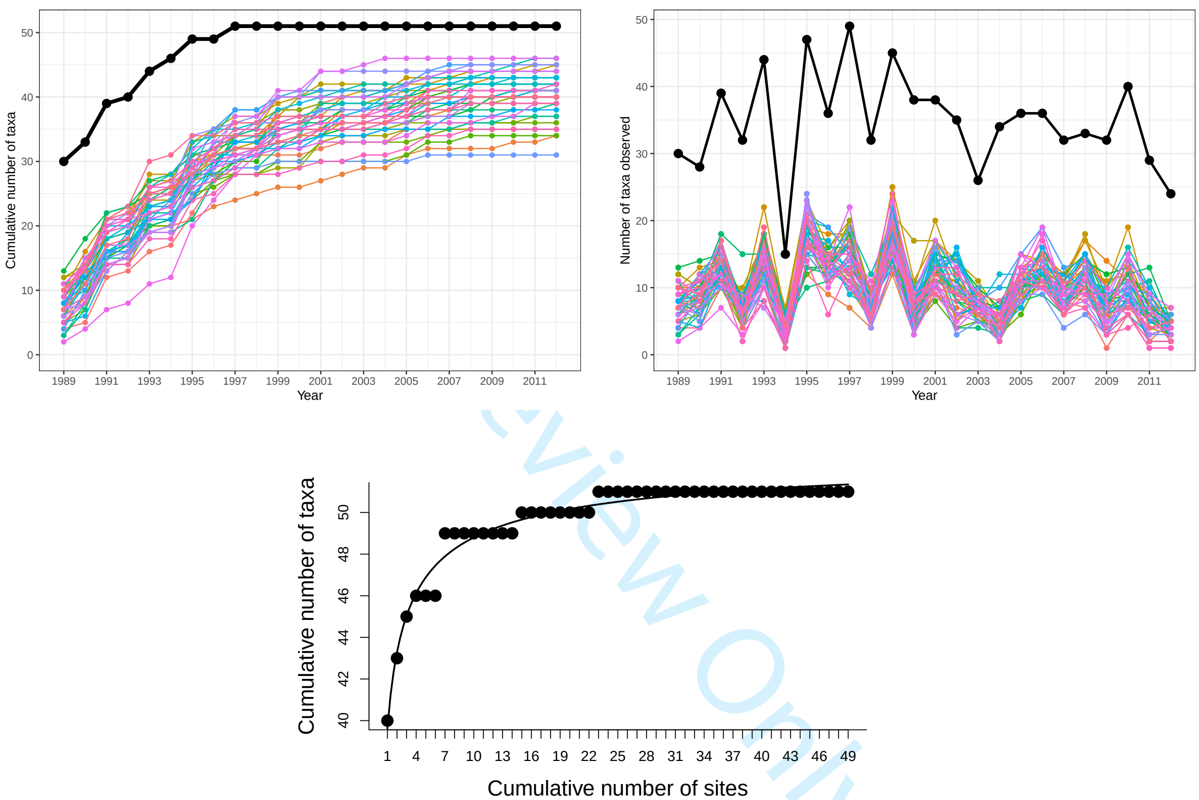

Figure S8: Temporal species accumulation curves (left), annual richness (right), and spatial species accumulation curve (lower) for 49 plots comprising the IBPE grassland community at Jornada LTER (1989-2012). The black lines represent total site-level values across all plots.

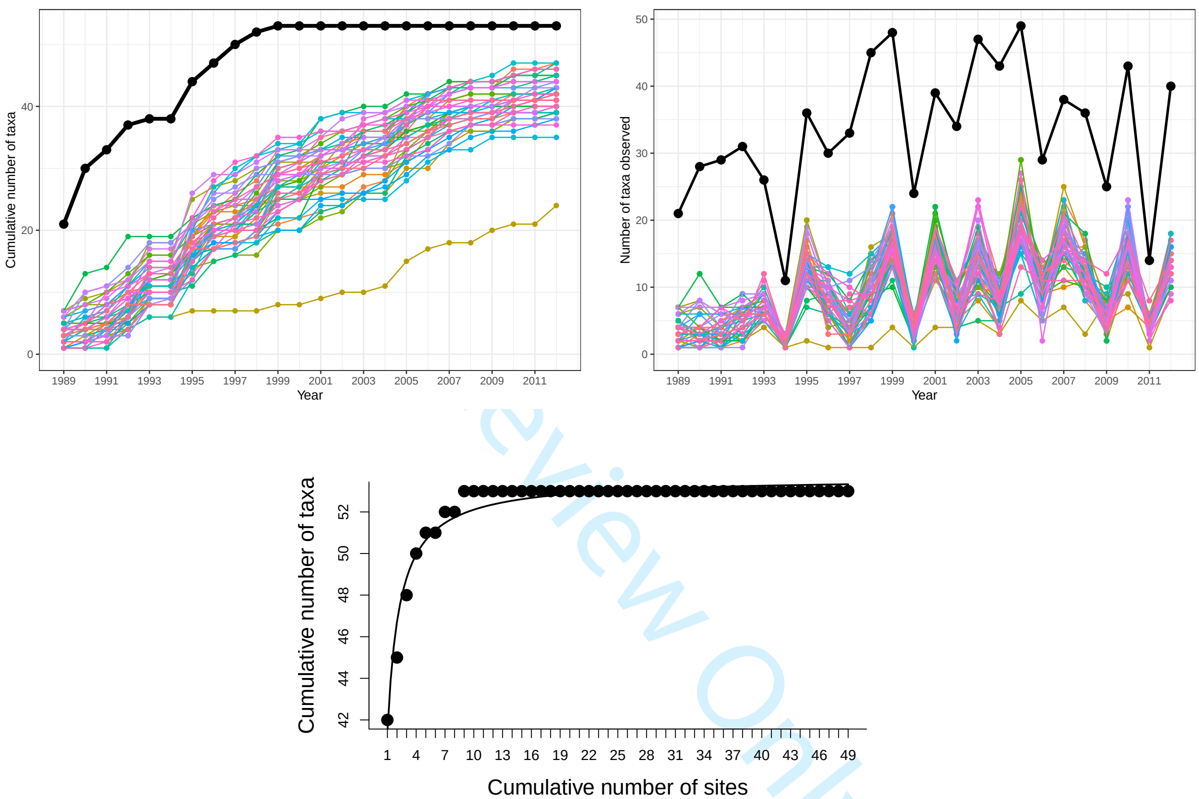

Figure S9: Temporal species accumulation curves (left), annual richness (right), and spatial species accumulation curve (lower) for 49 plots comprising the Summerford Mountain (SUMM) grassland community at Jornada LTER (1989-2012). The black lines represent total site-level values across all plots.

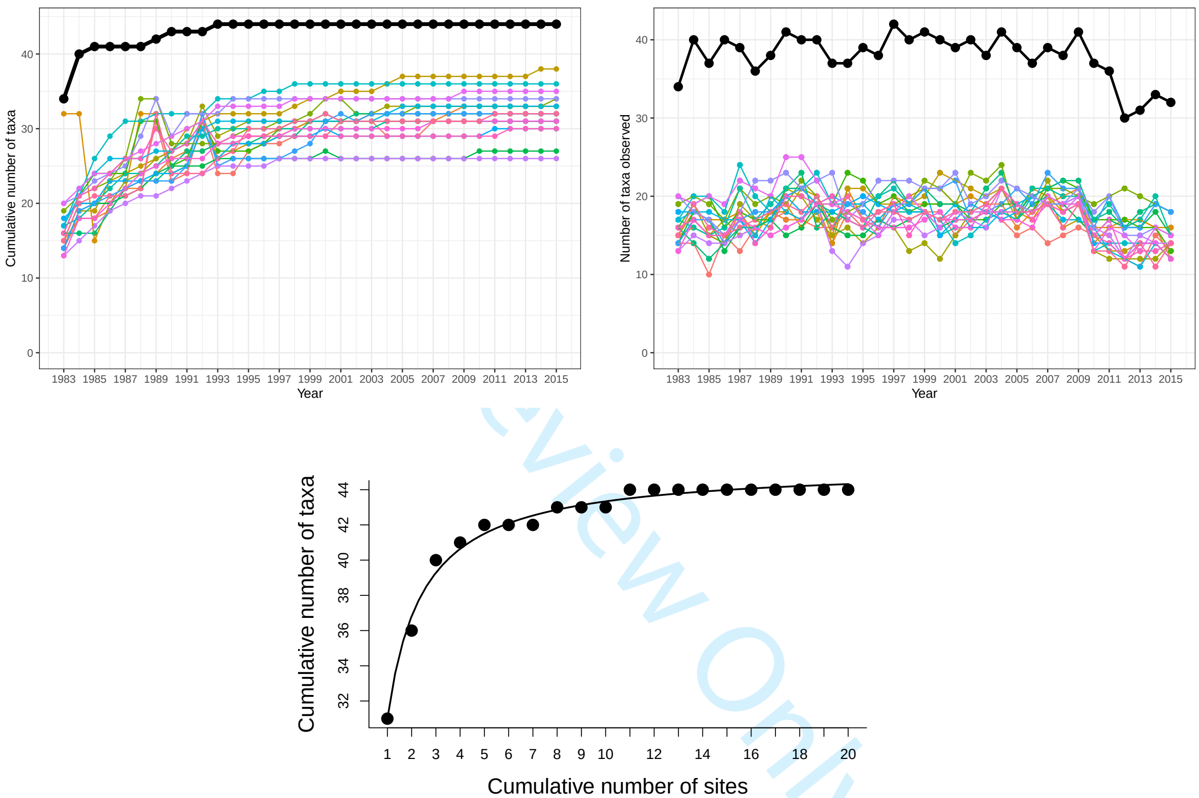

Figure S10: Temporal species accumulation curves (left), annual richness (right), and spatial species accumulation curve (lower) for 40 plots comprising fertile, nonrocky tully (lowland) soil habitats at Konza LTER (1983-2015). The black lines represent total site-level values across all plots.

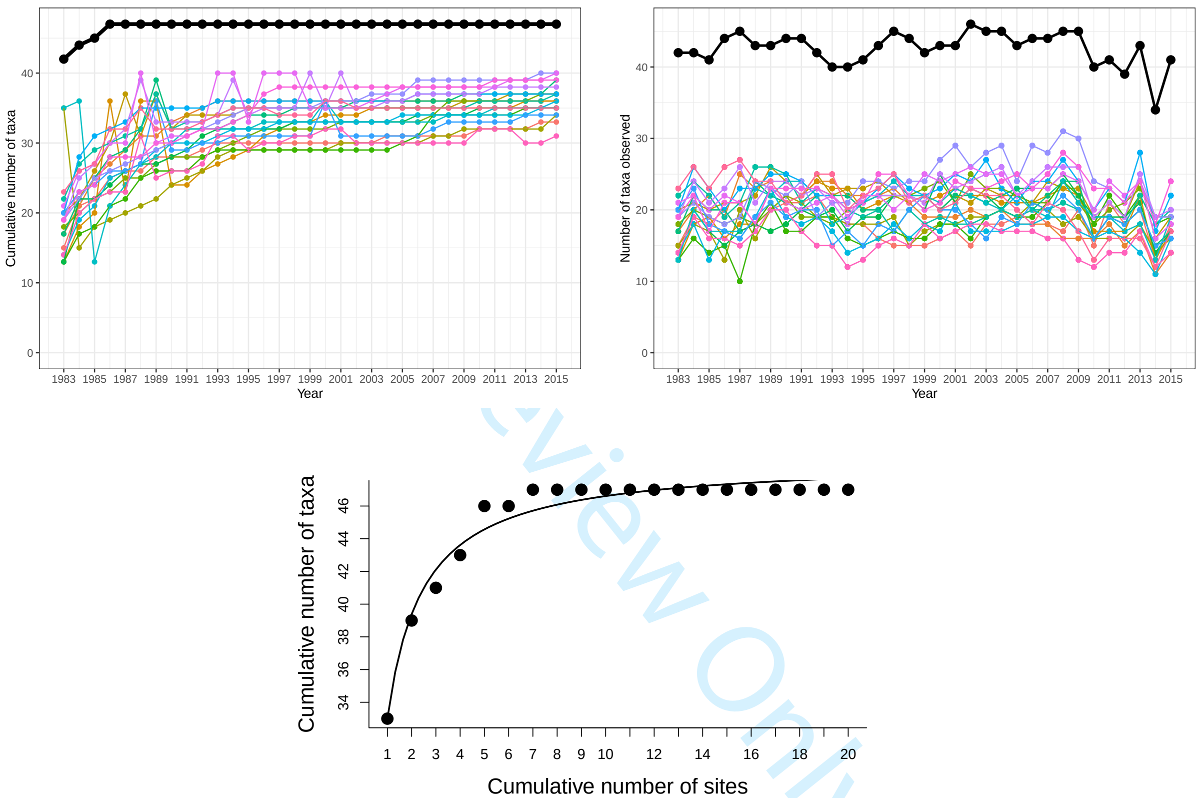

Figure S11: Temporal species accumulation curves (left), annual richness (right), and spatial species accumulation curve (lower) for 40 plots comprising the shallow, rocky florence (upland) soil habitat at Konza LTER (1983-2015). The black lines represent total site-level values across all plots.

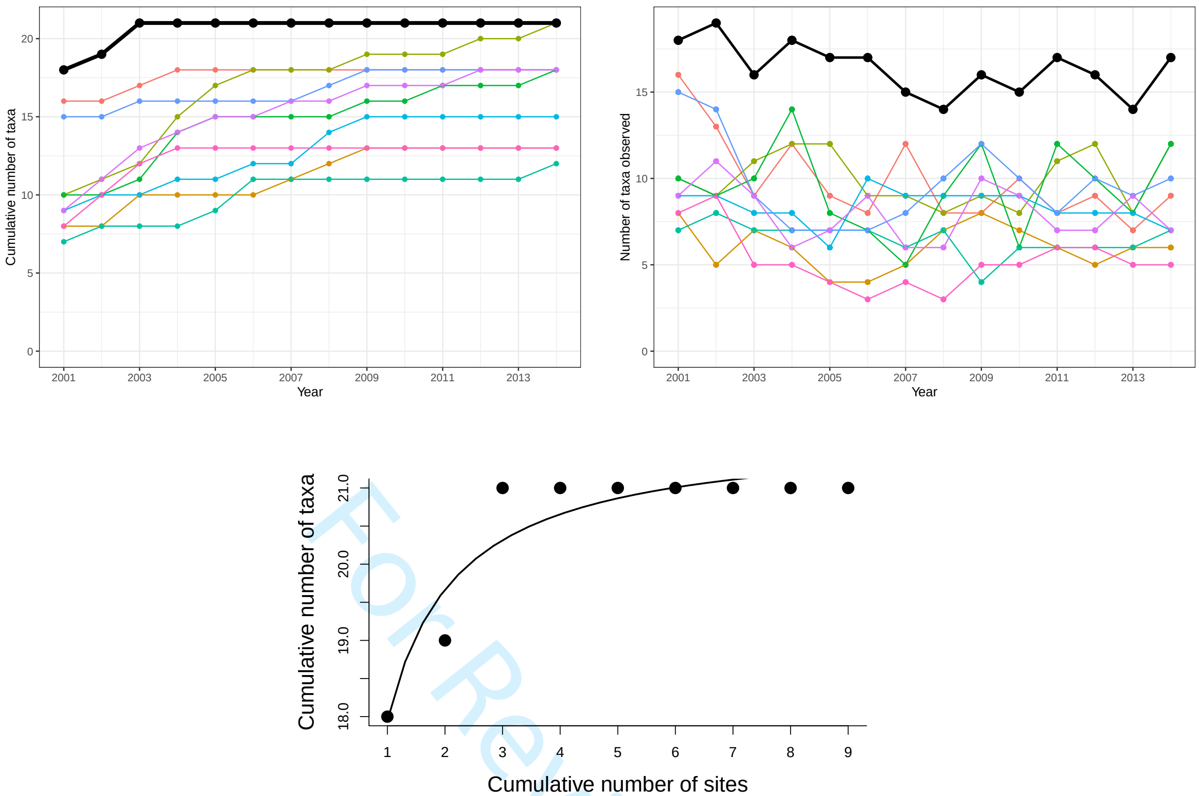

Figure S12: Temporal species accumulation curves (upper left), annual richness (upper right), and spatial species accumulation curve (lower) for 9 Maui, Hawaii corals plots (1999-2015). The black lines represent total site-level values across all plots.

S1.6 Maui, Hawaii (MAU)

Data on the percent cover of corals in Maui, Hawaii were downloaded from the U.S. Geological Survey (Guest et al., 2018). At each of 9 sites, coral cover was estimated annually (1999-2014) within ten 10-m transects using 20 photoquadrats per transect (bottom area = 0.34 m^2). Photoquatrats were not permanent, and cover was aggregated to the site scale. Data are shown in Figure S12.

S1.7 Moorea Coral Reef (MCR)

Data on the percent cover of coral and algae taxa in three different reef habitats the Moorea Coral Reef LTER were downloaded from EDI (Moorea Coral Reef LTER and Carpenter, 2015; Moorea Coral Reef LTER and Edmunds, 2018). At each of 30 sites, coral cover was estimated annually (2006-2015) within one permanent 40-m transect at each site using 40 photoquadrats per transect

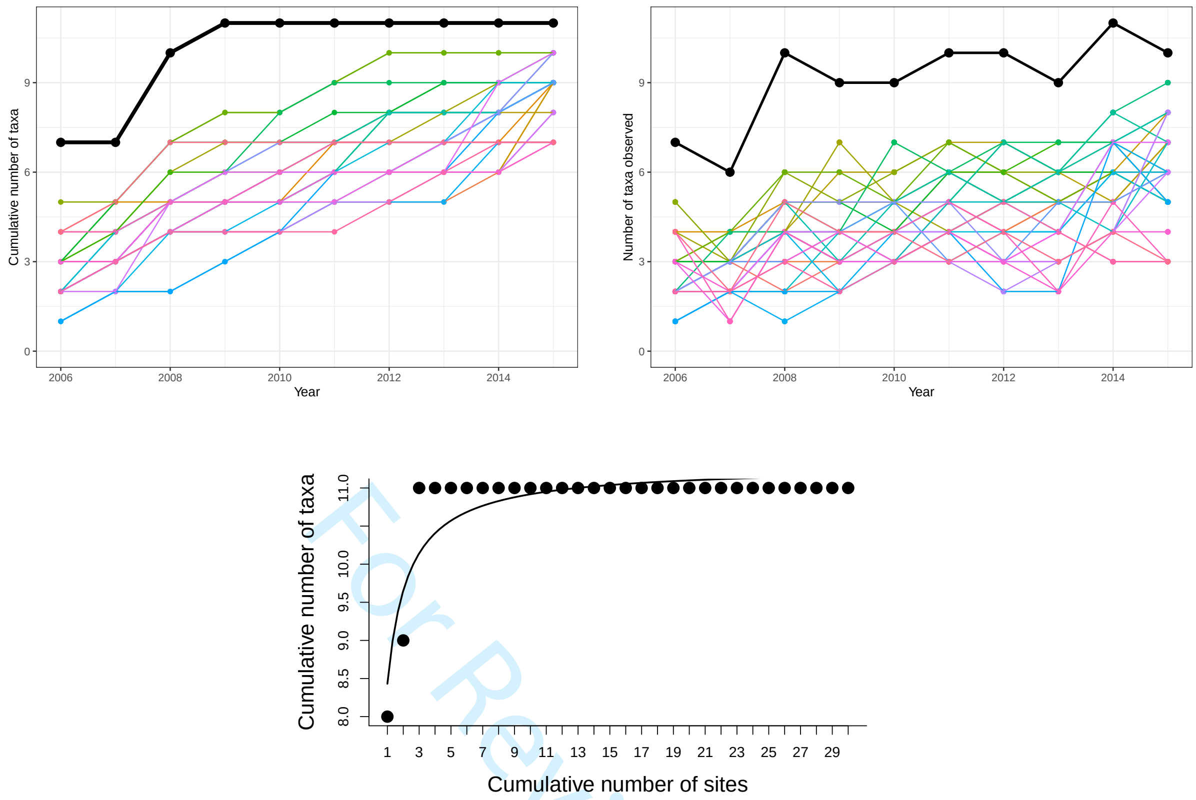

Figure S13: Temporal species accumulation curves (left), annual richness (right), and spatial species accumulation curve (lower) for the backreef habitat at Moorea Coral Reef (2006-2015). The black lines represent total site-level values across all plots.

(bottom area = 0.25 m^2). Each site represented one of three possible habitats (back reef, fringing reef, and outer reef). The data are shown from the back, fringing, and outer reef habitats in Figures S13, S14, and S15, respectively.

S1.8 Santa Barbara Coastal (SBC)

Annual estimates of biomass of all macroalgal taxa in kelp forests in the Santa Barbara Coastal LTER were downloaded from EDI (Santa Barbara Coastal LTER and Reed, 2018). At each of 11 sites, macroalgal density or cover was surveyed within 2-8 permanent transects per site (2 m wide by 40 m long) (Harrer et al., 2013; Reed et al., 2016). Abundance and size were converted to dry biomass using taxon-specific relationships developed for the study region (Harrer et al., 2013; Reed et al., 2016; Rassweiler et al., 2018). Data are shown in Figure S16.

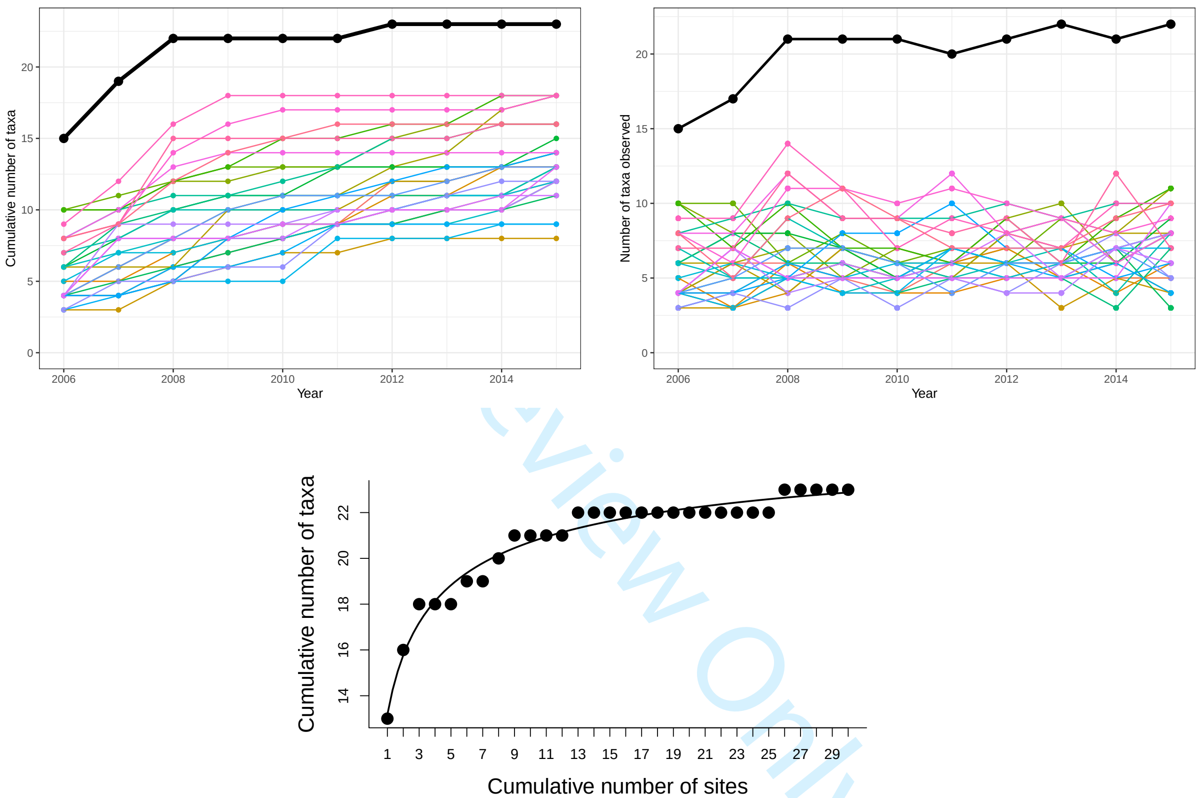

Figure S14: Temporal species accumulation curves (left), annual richness (right), and spatial species accumulation curve (lower) for algal and coral taxa in the fringing habitat at Moorea Coral Reef (2006-2015). The black lines represent total site-level values across all plots.

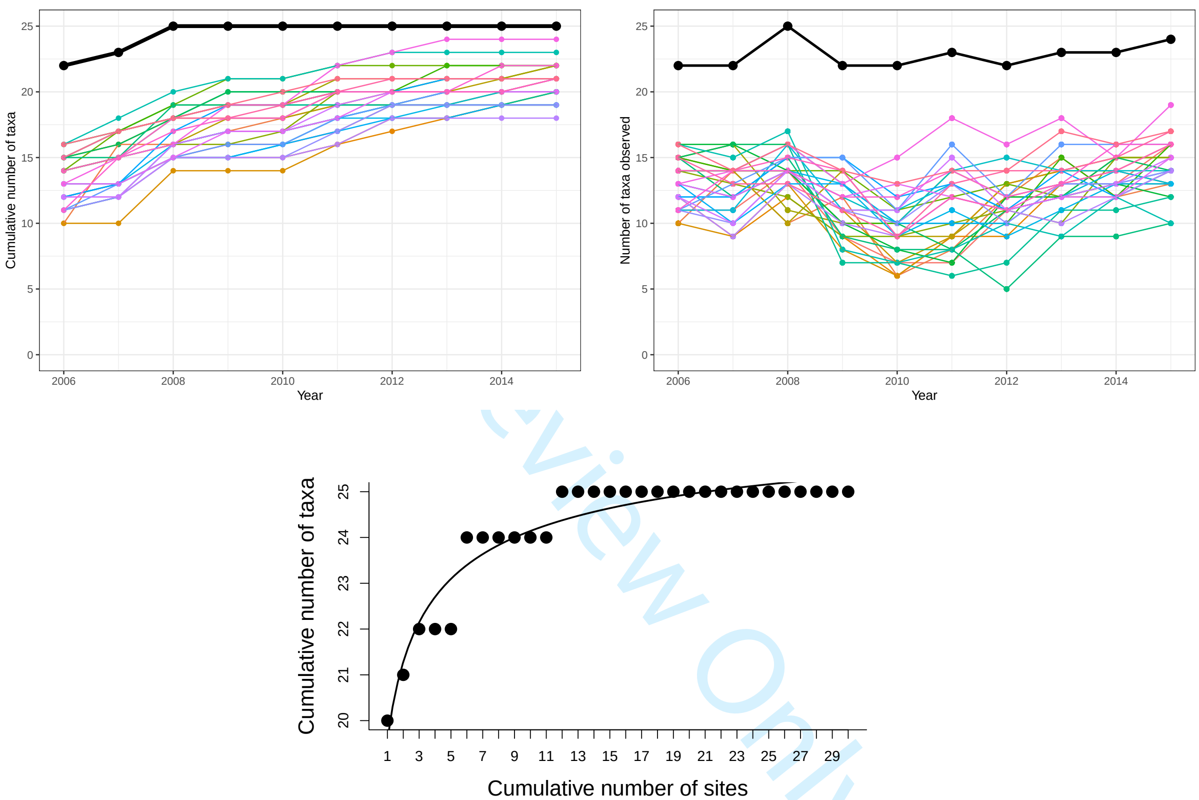

Figure S15: Temporal species accumulation curves (left), annual richness (right), and spatial species accumulation curve (lower) for algal and coral taxa in the outer (10 m depth) habitat at Moorea Coral Reef (2006-2015). The black lines represent total site-level values across all plots.

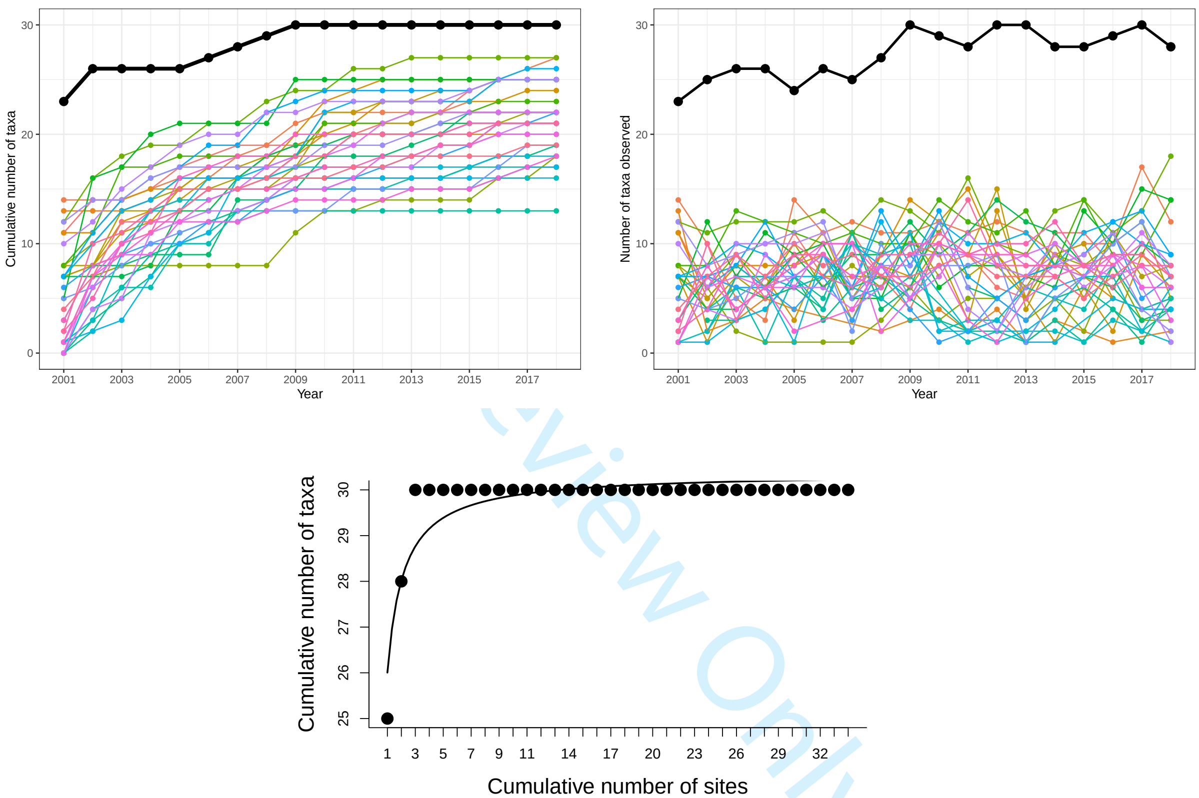

Figure S16: Temporal species accumulation curves (left), annual richness (right), and spatial species accumulation curve (lower) for sessile invertebrate and algal taxa at 34 plots at Santa Barbara Coastal LTER. The black lines represent site-level values.

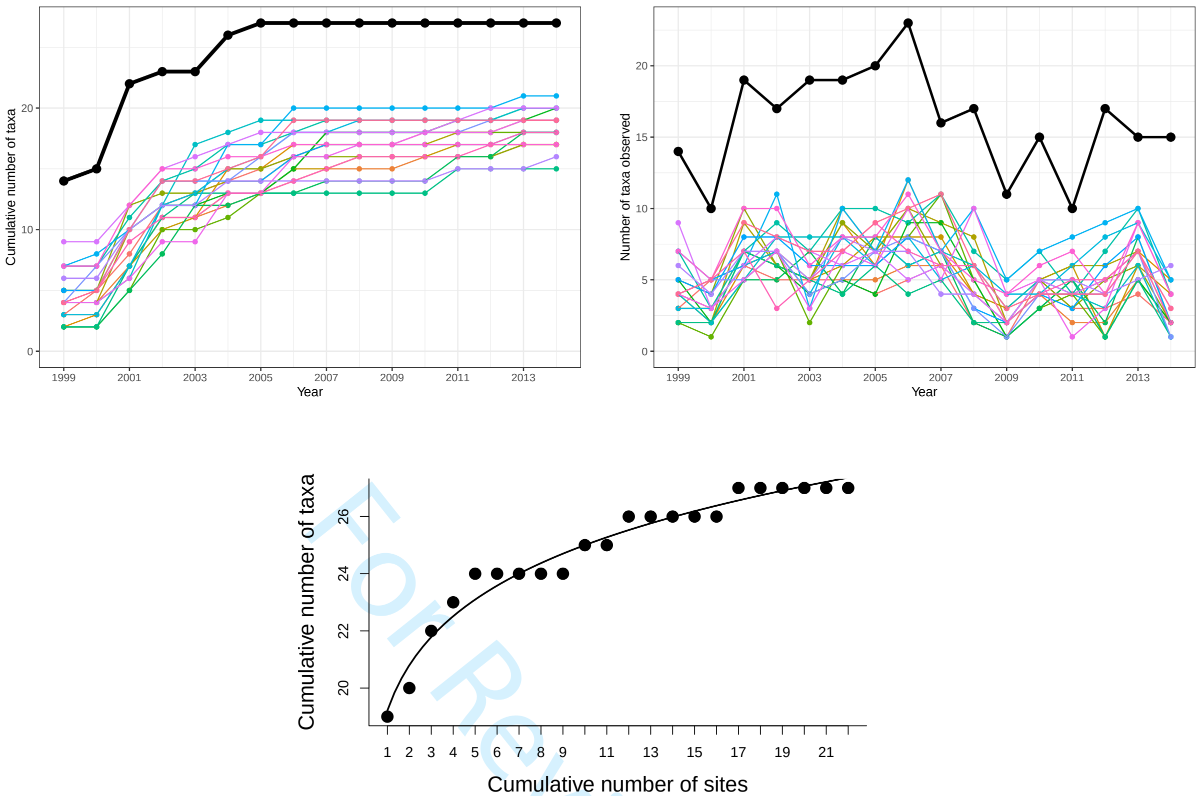

Figure S17: Temporal species accumulation curves (left) and annual richness (right), and spatial species accumulation curve (lower) in the black grama habitat at Sevilleta LTER. The black lines represent total site-level values across all plots.

S1.9 Sevilleta (SEV)

Data were downloaded from EDI (Muldavin and Moore, 2016). Three ecosystem types were included: black gamma (G), creosote(C) and blue gramma (B) (Figures S17, S18, and S19). Methods are described in (Muldavin et al., 2008) and (Rudgers et al., 2018). Within the black gramma community (G), the 22 plots that were sampled annually between 1999-2014 were included. Within the creosote community (C), the plots that were sampled annually between 1999-2014 were included. The G and C communities are about 0.5 km apart. Within the blue gramma community (B), 42 taxa at 30 plots sampled annually between 2002-2014 were included.

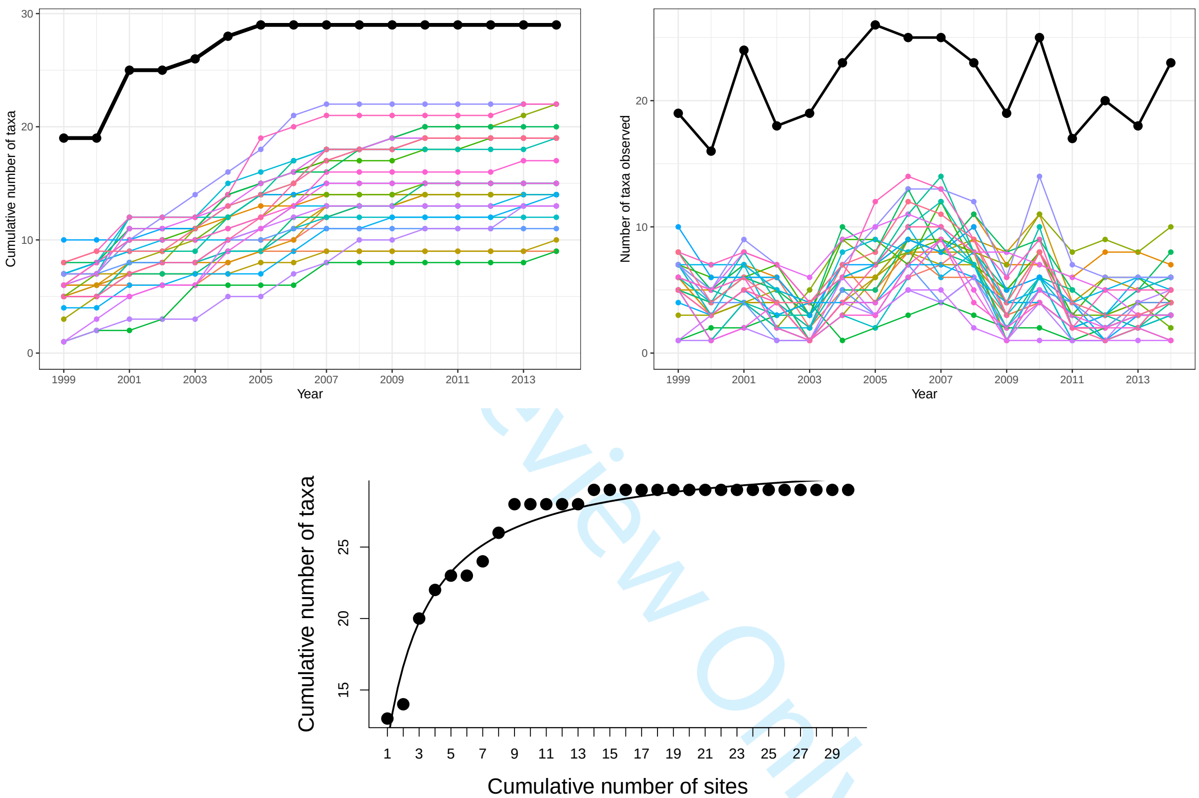

Figure S18: Temporal species accumulation curves (left) and annual richness (right), and spatial species accumulation curve (lower) in the creosote habitat at Sevilleta LTER. The black lines represent total site-level values across all plots.

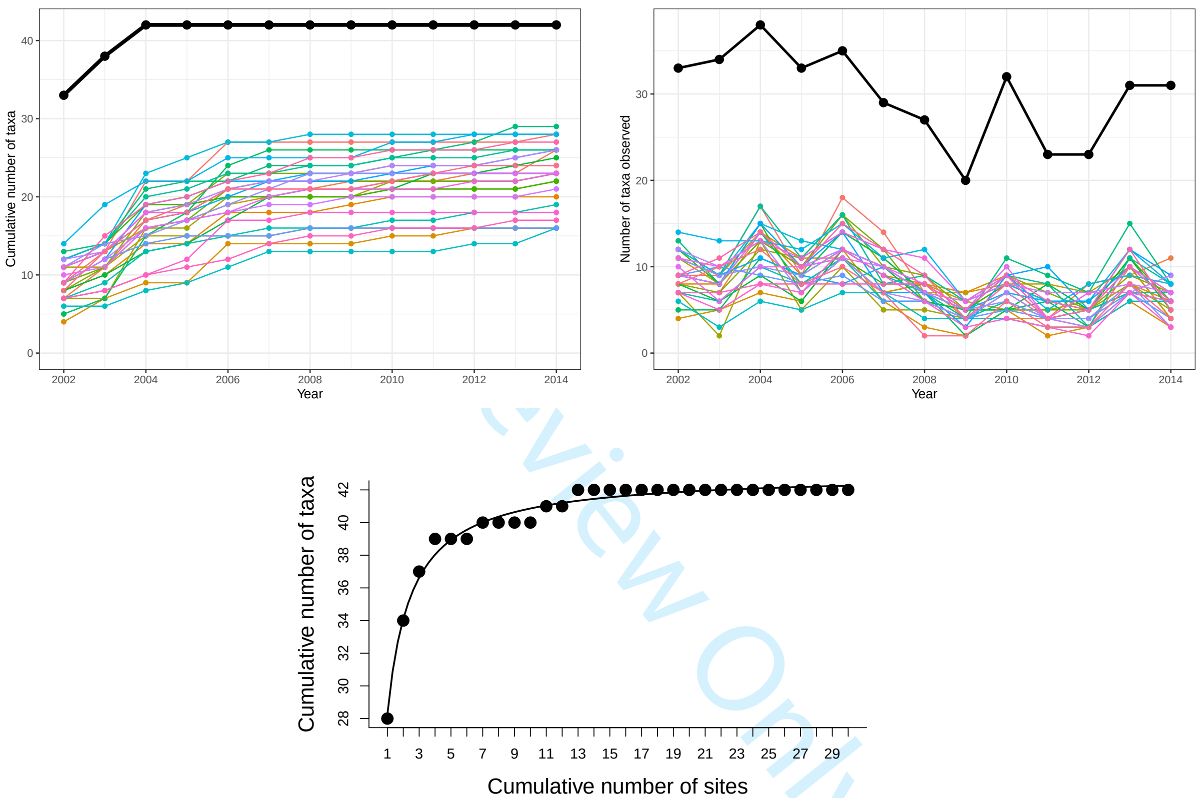

Figure S19: Temporal species accumulation curves (left) and annual richness (right), and spatial species accumulation curve (lower) in the blue grama habitat at Sevilleta LTER. The black lines represent total site-level values across all plots.

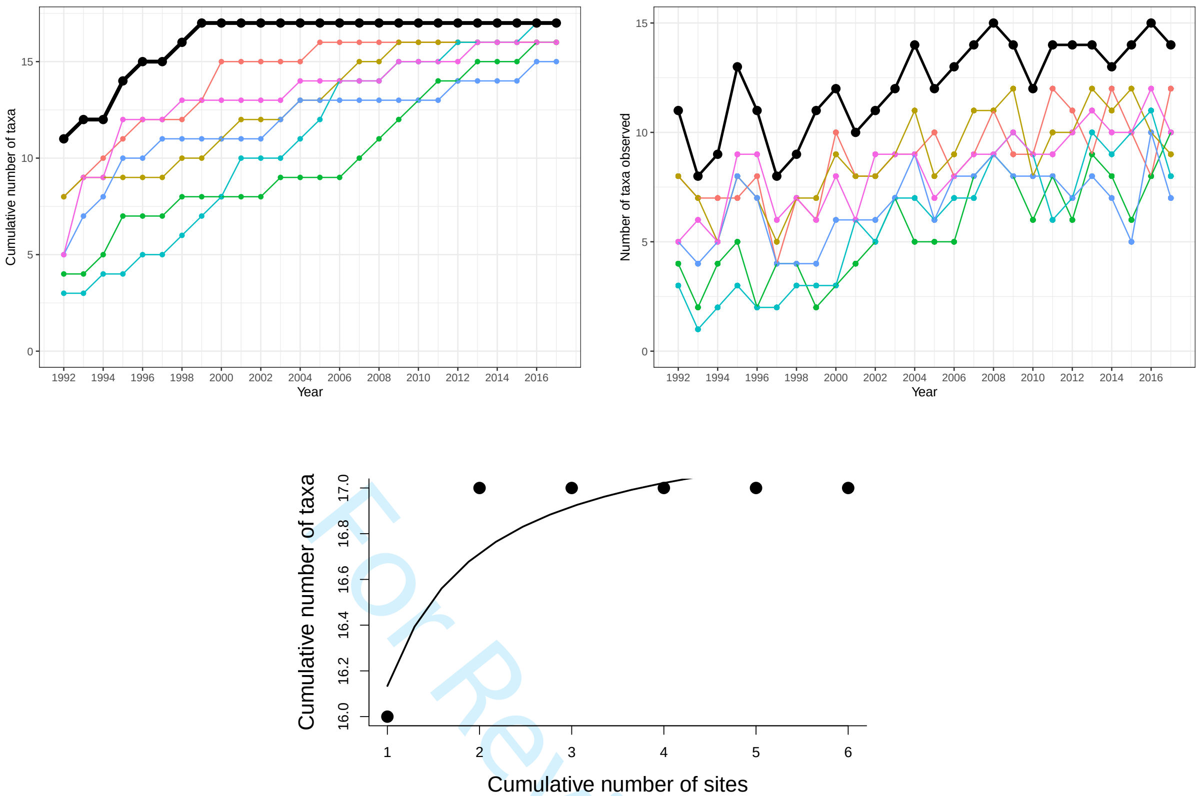

Figure S20: Temporal species accumulation curves (left), annual richness (right), and spatial species accumulation curve (lower) for coral taxa at CSUN US Virgin Islands research site. The black lines represent site-level values.

S1.10 US Virgin Islands National Park (USVI

Data on the percent cover of Scleractinian corals at St. John in the US Virgin Islands were downloaded from EDI (Edmunds, 2019). At each of 6 sites, Coral cover was estimated using 18-40 photoquadrates (bottom area = 0.25 m^2). Corals were identified to the genus level. Quadrats were not permanent, and abundance was aggregated to the site scale. Data are shown in Figure S20.

S2 Statistical significance of richness synchrony

Table S1: The degree of spatial synchrony in species richness (r) and its associated p-value, for 20 empirical metacommunity datasets.

Dataset	r	p
DRT	0.054	0.177
HAY	0.396	< 0.001
JRG	0.348	< 0.001
JRN_BASN	0.760	< 0.001
JRN_IBPE	0.775	0.001
JRN_SUMM	0.810	< 0.001
KNZ_UP	0.389	< 0.0001
KNZ_LOW	0.472	< 0.001
LOK	0.519	< 0.001
MAU	0.089	0.052
MCR_BACK	0.089	< 0.001
MCR_FRNG	0.057	0.005
MCR_OUT	0.442	< 0.001
MDK	0.236	0.001
SBC	0.053	< 0.001
SEV_B	0.640	< 0.001
SEV_C	0.611	< 0.001
SEV_G	0.602	< 0.001
UPK	0.392	< 0.001
USVI	0.269	< 0.001

S3 Relationships between stability and community variables

Table S2: Linear regression relationships between stability and community variables, in simulated and empirical metacommunities. Stability is measured as the CV over time of total biomass or percent cover.

	Simulated		Empirical	
Predictor	β	R^2	β	R^2
Richness synchrony	0.279	0.48	0.575	0.43
Richness	-0.0006	0.02	-0.019	0.13
Evenness	-0.748	0.06	-0.745	0.18
β-diversity	-0.840	0.02	-0.744	0.16
Turnover rate	3.676	0.10	1.029	0.49
Mean spatial synchrony			0.921	0.34

S4 Results from alternate model formulation

All following figures have identical formatting to those in the main text; the difference between these results and those presented in the main text is that, here, in simulations dispersal takes place after population growth. For results presented in the main text, dispersal takes place prior to population growth. Results are largely consistent regardless of the order of dispersal.

Specifically, within a patch, p, the abundance N of each species s changes through time t according to:

$$N_{s,p,t+h} = N_{s,p,t} \exp[r_s(1 - \frac{N_{s,p,t}}{K_s} - \sum_{j \neq s} \frac{\beta_{s,j} N_{j,p,t}}{K_j}) + \sigma_{e,s}\mu_{e,p,t} + \frac{\sigma_{d,s}\mu_{d,s,p,t}}{\sqrt{N_{s,p,t}}}], \tag{1}$$

where the time step $t+h$ denotes an intermediate time step after time t where dispersal has not yet occurred between patches. In the above equation, r is a species' intrinsic (density-independent growth rate), K is its carrying capacity in a patch, and $\beta_{s,j}$ is the competition coefficient of species j on species s. Model parameters and their values are given in Table **??**. The competition coefficient $\beta_{s,j}$ is related to the α coefficients of Lotka-Volterra dynamics where $\beta_{s,j} = \alpha_{s,j}K_j/K_s$ (Loreau and de Mazancourt, 2013).

Here, $\sigma_{d,s}$ is the susceptibility of species s to demographic fluctuations and $\mu_{d,s,p,t}$ are independent, identically distributed normal variables with mean zero and variance one representing fluctuations through time for each species in each patch.

Environmental stochasticity is incorporated through $\mu_{e,p,t}$, which represents environmental variation in each patch through time and $\sigma_{e,s}$, which quantifies the impact of environmental variation on each species s. While Loreau and de Mazancourt (2013) restricted $\mu_{e,p,t}$ to be uncorrelated, here we extend their model to allow for temporal autocorrelation in environmental conditions and variation across patches. To do so, we follow the formulation from Ripa and Lundberg (1996), where we first create a time series of regional climate conditions, c:

$$c_{t+1} = ac_t + b\phi_t. \tag{2}$$

We set the initial condition $c_0 = 0$. In eqn 2, a controls the temporal autocorrelation of the climate where $a = 0$ represents uncorrelated, white noise. When $a > 0$ temporal environmental variation exhibits positive autocorrelation (Ripa and Lundberg, 1996), where successive events are more likely to be similar to other events that occur closely in time. Stochastic noise $\phi_t \sim Normal(0, 1)$ is scaled by the magnitude of its effect, b. Following Ripa and Lundberg 1996, $b = (1-a^2)^{0.5}$, which restricts $var(c)$ to be the same for all autocorrelation (a values) considered. From the time series of regional climactic conditions, we create between-patch variation that represents the degree of microhabitat variation (Ford et al., 2013; Gómez-Aparicio et al., 2005). To do so, $\mu_{e,p,t} \sim Normal(c_t, h)$ where h controls the variability between patches.

Immediately following local dynamics, global dispersal between patches occurs, such that a species has an equal probability of dispersing to any patch in the metacommunity. Abundance after both growth and dispersal is indexed as time step $t + 1$, and is

$$N_{s,p,t+1} = N_{s,p,t+h} - d_s N_{s,p,t+h} + d_s \sum_{x \neq p} \frac{N_{s,x,t+h}}{P-1}, \tag{3}$$

where P denotes the total number of patches in the metacommunity, and d_s is a species' stochastic dispersal rate, which is distributed according to a binomial distribution. This approach is equivalent to modeling dispersal as a multinomial distribution with probabilities of $1 - d_s$ of not dispersing and $d_s/(p-1)$ of dispersing to a patch $x = 1...P$ such that $x \neq p$ (Shoemaker and Melbourne, 2016).

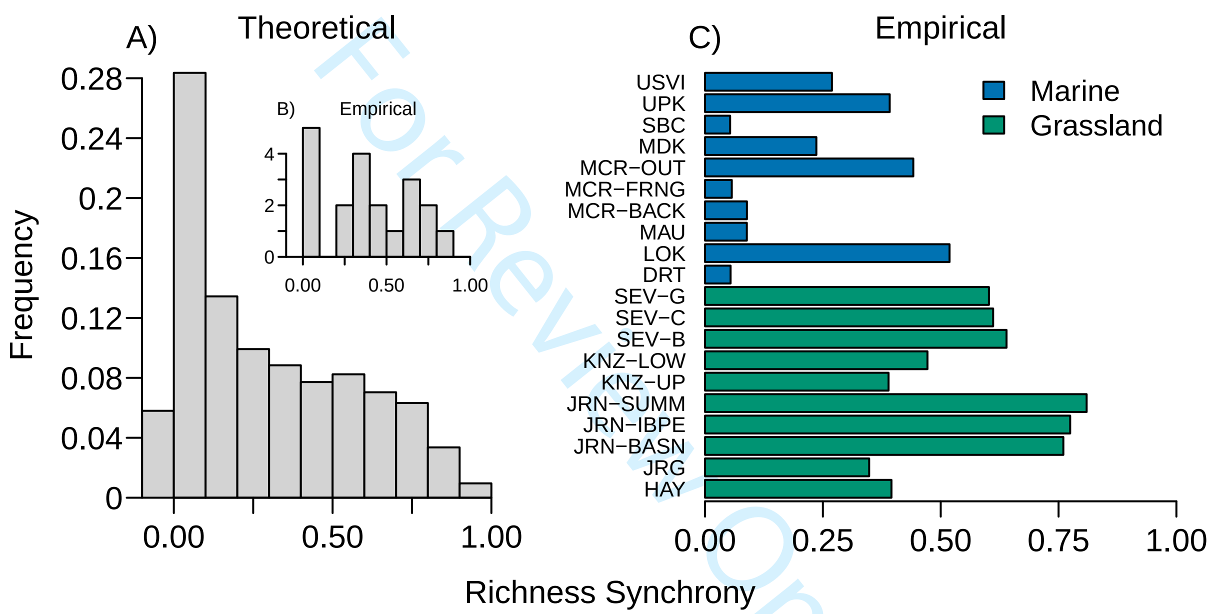

Figure S21: Spatial synchrony in species richness in (A) 2500 simulated and (B, C) 20 empirical metacommunities.

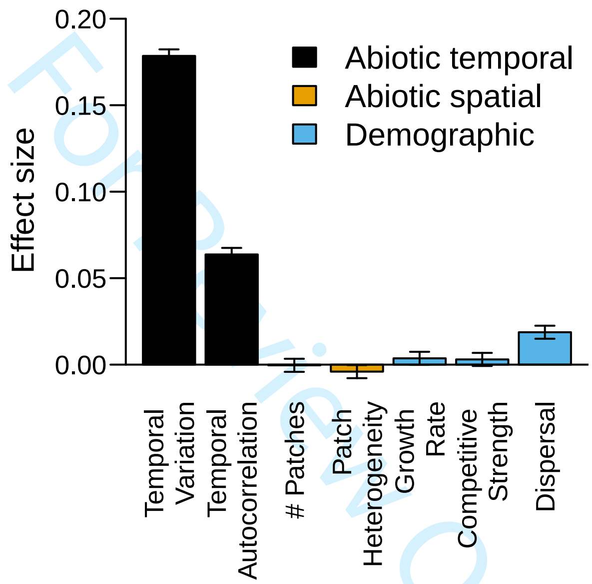

Figure S22: Effect sizes of variation in model parameters on the degree of spatial synchrony of richness in simulated metacommunities. Effect sizes are linear regression coefficients on standardized predictors. Error bars indicate 1 standard error.

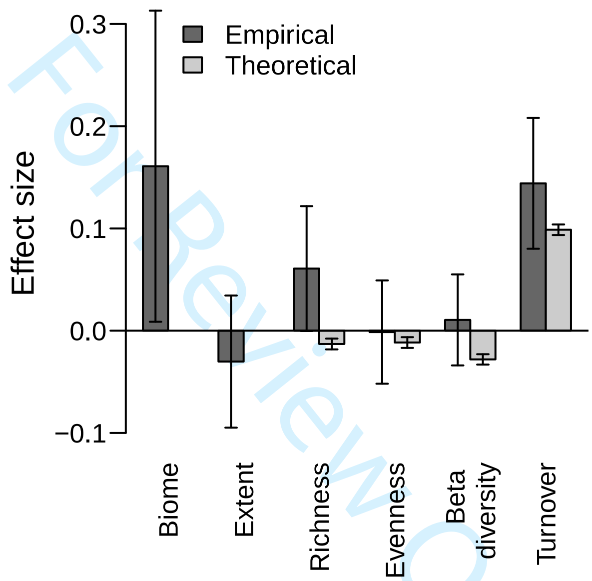

Figure S23: Effect sizes of variation in attributes of empirical and theoretical metacommunities on spatial synchrony of richness. Effect sizes are linear regression coefficients on standardized predictors. There is no direct analog of biome or extent in our theoretical simulations, so no bar is drawn. Error bars indicate 1 standard error.

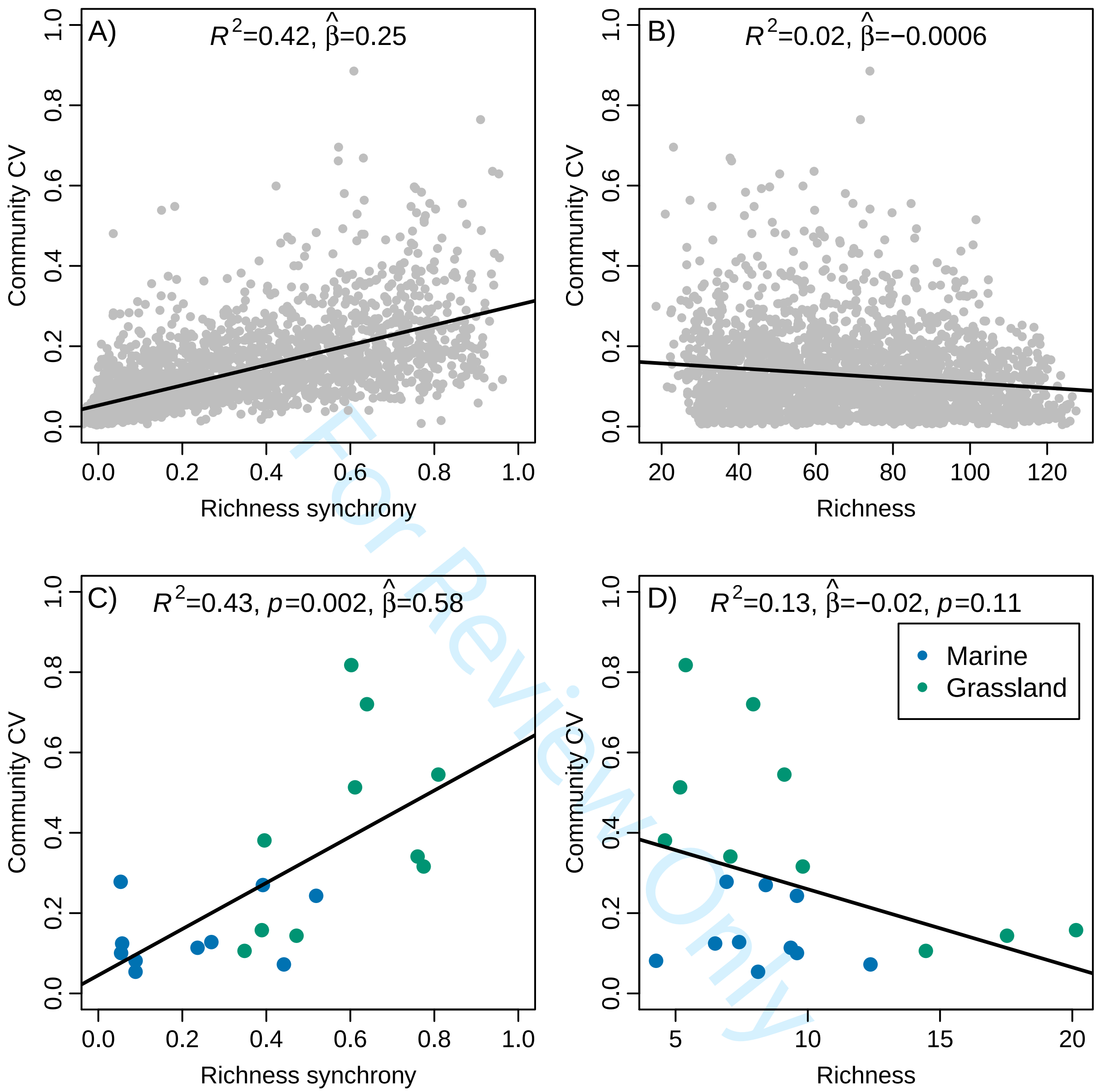

Figure S24: Richness synchrony is related to (in)stability of ecosystem function in theoretical (A) and empirical (C) metacommunities, and more strongly so than species richness itself in both theoretical (B) and empirical (D) metacommunities. The community CV is measured, for simulations, as the cv of total abundance, and for empirical datasets as the coefficient of variation of total biomass or total cover, depending on units of the underlying data.

References

Adler, P. B., Tyburczy, W. R., and Lauenroth, W. K. (2007). Long-term mapped quadrats from kansas prairie: demographic information for herbaceous plants. *Ecology*, 88:2673.

Ford, K. R., Ettinger, A. K., Lundquist, J. D., Raleigh, M. S., and Lambers, J. H. R. (2013). Spatial heterogeneity in ecologically important climate variables at coarse and fine scales in a high-snow mountain landscape. *PloS One*, 8(6):e65008.

Gómez-Aparicio, L., Gómez, J. M., and Zamora, R. (2005). Microhabitats shift rank in suitability for seedling establishment depending on habitat type and climate. *Journal of Ecology*, 93(6):1194–1202.

Guest, J. R., Edmunds, P. J., Gates, R. D., Kuffner, I. B., Brown, E. K., Rodgers, K. S., Jokiel, P. L., Ruzicka, R. R., Colella, M. A., Miller, J., Atkinson, A., Feeley, M. W., and Rogers, C. S. (2018). Time-series coral-cover data from Hawaii, Florida, Mo'orea, and the Virgin Islands. U.S. Geological Survey data release. doi: 10.5066/F78W3C7W.

Harrer, S. L., Reed, D. C., Holbrook, S. J., and Miller, R. J. (2013). Patterns and controls of the dynamics of net primary production by understory macroalgal assemblage in giant kelp forests. *Journal of Phycology*, 49:248–257.

Hartnett, D. C. and Collins, S. L. (2016). PVC02 plant species composition on selected watersheds at konza prairie ver 7. Environmental Data Initiative. https://doi.org/10.6073/pasta/2871559b94adabdbd79c97d99905ee6d.

Hobbs, R. J. and Mooney, H. A. (1985). Community and population dynamics of serpentine annual grassland in relation to gopher disturbances. *Oecologia*, 67:342–351.

Loreau, M. and de Mazancourt, C. (2013). Biodiversity and ecosystem stability: a synthesis of underlying mechanisms. *Ecology letters*, 16:106–115.

Moorea Coral Reef LTER and Carpenter, R. (2015). MCR LTER: Coral reef: Long-term population and community dynamics: Benthic algae and other community components, ongoing since 2005 ver 28. Environmental Data Initiative. https://doi.org.10.6073/pasta/79a6edbcf3aa2380d43deed778856416.

Moorea Coral Reef LTER and Edmunds, P. (2018). MCR LTER: Coral reef: Long-term population and community dynamics: Corals, ongoing since 2005 ver 35. Environmental Data Initiative. https://doi.org/10.6073/pasta/263faa48b520b7b2c964f158c184ef96.

Muldavin, E. and Moore, D. (2016). Core research site web seasonal biomass and seasonal and annual NPP data for the net primary production study at the sevilleta national wildlife refuge, new mexico (1999-present) ver 244946. Environmental Data Initiative. https://doi.org/10.6073/pasta/b913c188d07335b3e88fd585c1cd20b5.

Muldavin, E. H., Moore, D. I., Collins, S. L., Wetherill, K. R., and Lightfoot, D. C. (2008). Aboveground net primary production dynamics in a northern Chihuahuan Desert ecosystem. *Oecologia*, 155:123–132.

Peters, D. and Huenneke, L. (2015). NPP study: Quadrat field measurement data ver 64. Environmental Data Initiative. https://doi.org/10.6073/pasta/d65a72899a4294bc9e5e64158a6dbeae.

Rassweiler, A., Reed, D. C., Harrer, S. L., and Nelson, J. C. (2018). Improved estimates of net primary production, growth and standing crop of *Macrocystis pyrifera* in southern california. *Ecology*, 99:2132–2132.

Reed, D., Washburn, L., Rassweiler, A., Miller, R., Bell, T., and Harrer, S. (2016). Extreme warning challenges sentinel status of kelp forests as indicators of climate change. *Nature Communications*, 7:13757.

Ripa, J. and Lundberg, P. (1996). Noise colour and the risk of population extinctions. *Proc. R. Soc. Lond. B*, 263(1377):1751–1753.

Rudgers, J. A., Chung, Y. A., Maurer, G. E., Moore, D. I., Muldavin, E. H., Litvak, M. E., and Collins, S. L. (2018). Climate sensitivity functions and net primary productivity: a framework for incorporating climate mean and variability. *Ecology*, 99:576–582.

Santa Barbara Coastal LTER and Reed, D. C. (2018). SBC LTER: Reef: Annual time series of biomass for kelp forest species, ongoing since 2000 ver 7. Environmental Data Initiative. https://doi.org/10.6073/pasta/d5fd133eb2fd5bea885577caaf433b30.

Shoemaker, L. G. and Melbourne, B. A. (2016). Linking metacommunity paradigms to spatial coexistence mechanisms. *Ecology*, 97:2436–2446.